Analytical Modeling and Equivalent Electromechanical Loading Techniques for Adaptive Laminated Piezoelectric Structures

by

Clayton L. Smith

Thesis submitted to the faculty of the
Virginia Polytechnic Institute and State University
in partial fulfillment of the requirements for the degree of

Master of Science
in
Mechanical Engineering

APPROVED:

Daniel J. Inman, Chairman

Eric M. Austin | Donald J. Leo

January, 2001
Blacksburg, Virginia

Keywords: Piezoelectric, Laminated, Finite Element

Analytical Modeling and Equivalent Electromechanical Loading Techniques for Adaptive Laminated Piezoelectric Structures

Clayton L. Smith

(ABSTRACT)

Many commercial finite element programs support piezoelectric modeling and composite modeling to some extent. The popular program ABAQUS, however, has piezoelectric modeling capabilities only for continuum and one-dimensional truss elements. In situations where aspect ratio constraints and computational inefficiencies become a significant issue, such as modeling very large thin structures, alternate modeling techniques are sometimes required. Much of the focus of this thesis was to introduce equivalent methods for modeling laminated piezoelectric beams and plates. Techniques are derived based on classical beam and plate theory, classical lamination theory, and the linear theory of piezoelectricity. Finite element approximations are used with the principle of minimum potential energy to derive the static equilibrium equations for piezoelectric laminated structures. Equivalent loading techniques are derived based on the constitutive equations of piezoelectricity to simulate actuation forces within the piezoelectric layers. Finite element models using equivalent modeling techniques as well as equivalent loading techniques for piezoelectric laminated structures are developed and compared to ABAQUS models, using piezoelectric elements, to evaluate the error in theoretical assumptions. The analysis will prove that equivalent structural models and equivalent loading techniques provide excellent means for simplifying the analysis of thin piezoelectric laminated structures.

Dedication

I dedicate this thesis in loving memory of my father, Dr. Clifford L. Smith Sr., who has always been very supportive, patient, understanding, and encouraging. It is of great sorrow that he is not able to share this with me.

I would also like to dedicate this to my mother, Carolyn Smith, for her continuous love, support, and encouragement through my academic years.

Acknowledgements

I would first like to thank God for making this possible. I would like to thank my parents, Clifford Sr. and Carolyn Smith, for their unconditional love, support, and encouragement. Thanks to my brother and sister, Clifford Jr. and Carla, for their support and motivation, especially throughout our childhood years. Thanks to my best friend, James Crawford, and brother-in-law, Wesley Stroble, for their words of encouragement.

A special thanks to my advisor, Prof. Daniel J. Inman, for providing support, encouragement, and for lending me the opportunity to work with such an intelligent group of individuals at CIMSS (Center for Intelligent Material Systems and Structures). Thanks to Prof. Eric M. Austin for his immeasurable contributions to this thesis. Thank you for all of your support, patience, motivation, and encouragement. Thanks to Prof. Donald J. Leo for the challenging homework assignments and contributions through coursework. Thanks to Greg Pettit and all of the students at CIMSS whom I have had the opportunity to work with. Finally, thanks to the faculty and staff at CIMSS for providing a family-oriented work environment.

This work was supported by Bekey Inc. under the direction of Ivan Bekey whom I would also like to thank.

Table of Contents

List of Figures

List of Tables

CHAPTER 1

Introduction

1.1 Problem Statement

Bekey Designs Inc. has developed a new concept for implementing very large, extremely low-weight optical sensing systems in space. The primary component of the system is an unsupported laminated reflector consisting of two layers of piezoelectric film, such as polyvinylindene fluoride (PVDF) in a bimorph configuration and a single layer of shape memory alloy (SMA), such as Nitinol. The structure will be coated with a reflective surface on one side to function as the primary reflector of a large telescope. The shape of the structure will be controlled in space by scanning an electron beam across the piezoelectric surface, causing local deformations at places where electron charges are deposited. The structure will not be tensioned by an auxiliary structure, so some actuation forces will be required to shape the structure into its desired shape in space. The dimensions of the structure are 25 meters in diameter, with a radius of curvature of 500 meters and a thickness of 25 microns. The structure will consists of two 10-micron layers of PVDF film bonded to a 4-micron Nitinol (SMA) film with a 1-micron reflective coating on the surface. The PVDF film will supply the adaptive corrective forces, while the Nitinol deploys the structure from an initial folded state.

Upon deployment in space, the Sun's heat will activate the Nitinol causing the membrane to deploy to its final configuration with minimal surface wrinkles. An electron beam will be made responsive to an optical figure sensor, observing the shape of the structure, and will stimulate the PVDF layers to correct surface wrinkles and control the curvature of the reflector.

Before the concept is implemented in space, the static and dynamic response of the structure must be evaluated. The purpose of the analysis is to predict the depth and area of the surface imperfections that can be corrected, based on various layer thickness configurations. Potential problems expected modeling the structure are

- Modeling the very large and extremely thin laminated structure when aspect ratio constraints become a significant issue.
- Modeling the structure when computational efficiency becomes a significant issue (i.e., layers requiring many elements for finite element analysis).
- Accounting for the electrical and mechanical characteristics of the PVDF layers.
- Predicting the static and dynamic response of the nonlinear structure.

Within this thesis, all of the issues will be addressed, and an attempt will be made to alleviate some of the potential problems by deriving equivalent methods for modeling thin piezoelectric laminated structures.

1.2 Objectives

The objective of this thesis is to facilitate the modeling of a very large, extremely thin, piezoelectric laminated structure. Many computer programs support piezoelectric analysis to some extent. Our target structure is extremely thin compared to its in-plane dimensions, and models must account for both elastic and piezoelectric layers. Solid elements, which have piezoelectric capability, prove problematic due to the large aspect ratios that result when modeling the entire structure. Therefore, equivalent piezoelectric laminated elements are needed to adapt equivalent mechanical loads to simulate actuation within the piezoelectric layers. The primary objective of this paper is to derive equivalent methods for modeling laminated piezoelectric structures. Analytical solutions will be derived based on theory to aid in the derivations of simplified models. Classical lamination theory of beams and plates will be studied to gain an understanding of laminated structures composed of varying material properties and layer thickness. The principle of minimum potential energy is used to derive the static equilibrium equations. Finite element methods will be used to approximate the solutions for laminated structures. The linear theory of piezoelectricity will be explored to gain an understanding of the electromechanical coupling effects within piezoelectric materials. Concepts from all of the theories and studies will be used to derive equivalent methods for modeling piezoelectric laminated structures. A secondary yet very important objective is to determine equivalent mechanical loading techniques to simulate piezoelectric actuation within the piezoelectric layers. Finally, equivalent-modeling techniques will be generated and compared to ABAQUS models to evaluate any errors in assumptions applicable to theoretical modeling.

In summary, the objectives are as follows:

1.) Derive mathematical models for laminated beams and plates, and compare results to ABAQUS finite element models.
2.) Derive mathematical models for piezoelectric beams and plates, and compare results to ABAQUS finite element models.
3.) Derive mathematical models for piezoelectric laminated beams and plates, and compare results to ABAQUS finite element models.
4.) Determine equivalent electromechanical loading conditions to simulate electrical actuation, and compare results to equivalent models subjected to equivalent mechanical loading conditions.

1.2.1 Overview

In the first chapter, the problem statements and objectives of this research are presented. The following section will consist of a review of past and present literature pertaining to the topic of this research. Chapter 2 consists of discussions on classical lamination theory, energy methods, finite element methods, and the linear theory of piezoelectricity. In chapter 3, finite element formulations are derived based on classical lamination theory, piezoelectric theory, and the principle of minimum potential energy. Also, equivalent loading techniques are derived for piezoelectric beams and plates by two methods, a technique similar to static condensation and a technique based on the constitutive equations of piezoelectricity. Chapter 4 consists of comparisons of analytical solutions with computer based finite element solutions. Multiple versus single layer modeling, piezoelectric modeling, piezoelectric laminate modeling and equivalent loading techniques are compared to ABAQUS results. Finally, in Chapter 5, a summary is given and conclusions are made based on the research.

1.3 Review of Literature

There have been many publications on analytical and finite element formulations for piezoelectric materials and structures (e.g., [1, 3, 5, 6, 9, 12, 16, 30, 31, 41]). None, however, specifically address the problem with modeling extremely thin laminated structures, nor, do any develop piezoelectric actuation by a surface charge using mechanical loading. Listed below are a few key references pertinent to this work.

Henno A., and Hughes, T. (1970) [10]

Henno and Huges derived tetrahedral piezoelectric elements for vibration analysis. They introduce the concept of "static condensation of the electric potential degrees of freedom," in which the electric potential and loads are written in terms of the mechanical properties of the structure. An advantage is that a system of equations is derived only in terms of the mechanical degrees of freedom. The study serves as a basis for electro-elastic finite element derivations for plates, shells, and axisymmetric solids. The derivations were introduced to illustrate principles and lay groundwork for piezoelectric finite element modeling.

Suleman, A., and Venkayya, V.B. (1995) [34]

Suleman and Venkayya developed finite element formulations for composite plates with laminated piezoelectric layers. They developed 24 degrees of freedom piezoelectric plate elements with one electrical degree of freedom per surface. They make assumptions that the electrical degrees of freedom were constant along the plane and vary linearly through the thickness of the piezoelectric layers. An advantage of their methodology is that the analysis eliminates problems associated with modeling thin plate elements with isoparametric solid elements, which have excessive shear strain energies and higher stiffness in the thickness directions.

They conclude that

1.) numerical results generated by the electromechanical finite element plate model agree well with experimental data and solid element formulations reported in literature.
2.) finite element models with one electrical degree of freedom per piezoelectric layer is much simpler to formulate and computationally more efficient than models based on solid element formulations, where the number of degrees of freedom used to model the problem are significantly larger.

Heyliger P., and Brooks S. (1996) [11]

Heyliger and Brooks present exact solutions for piezoelectric laminates in cylindrical bending. The paper demonstrates limitations of simplified theories in making approximations for through-the-thickness elastic and electric fields. The solutions provide a means of comparisons to assess relative accuracies, advantages, and disadvantages of more computationally efficient models based on theory.

Saravanos D.A., Heyliger, P.R., and Hopkins, D.A. (1997) [31]

Saravanos, Heyliger, and Hopkins develop discrete layer (layerwise) theories for dynamic analysis of piezoelectric composite plates. The theory utilizes piecewise continuous approximations through the thickness of the laminate for both displacements and electric potentials. Advantages of layerwise approaches are that they capture intra-laminar and inter-laminar effects in elastic (Reddy, 1987) and elastodynamic (Saravanos, 1993, 1994) problems of composite plates. Other advantages are that each layer is modeled using independent approximations for the in-plane displacement components and electro-static potential in a unified representation, as mandated by the linear theory of piezoelectricity. They also perform "static condensation of the electric potential degrees of freedom," in which the electric potential and loads are written in terms of the mechanical properties. Finite element models were compared to exact solutions verifying the capability of the layerwise mechanics to model free vibration of piezoelectric composite plates.

Saravanos, D.A. (1997) [30]

Saravanos developed finite elements that enable the formal analysis of piezoelectric composite shells. His methodology was based on what is called a "Mixed Laminate Theory." This theory utilizes unique approximations for displacements and electric potentials. The first order shear deformation theory was assumed on the mechanical displacements, while discrete layer ("layerwise") approximations are assumed on the electrical potentials. The advantages of this mixed laminate theory are they

1.) accurately and efficiently model thin and/or moderately thick laminated piezoelectric shells with arbitrary laminations and electric configurations, and they
2.) capture the through-the-thickness electric heterogeneity induced by the embedded piezoelectric layers.

Finite element methods were compared to exact solutions [Heyliger, Saravanos (1995)]. The analysis was justified with excellent convergence and agreement with fundamental frequencies and through-the-thickness electromechanical modes of moderately thin plates.

Bhattacharya, P., Suhail H., and Sinha, P.K. (1998) [3]

Bhattacharya, Suhail, and Sinha developed quadratic isoparametric piezoelectric elements to study the effects of stacking sequence, geometric boundary conditions, and applications of electrical voltages on the free vibration frequencies. They report that applications of electrical voltages and boundary conditions produce significant changes in the free vibration frequencies. They conclude that cantilevered beams have frequencies significantly higher than simply supported or clamped beams subjected to actuating voltages. They also conclude that the effects of in-plane stress on the overall stiffness are higher as compared to bending stress with applications of electric loading.

Huang, Y-Q, M Liu, and C-C Wu (1999) [12]

Huang, Liu, and Wu investigated the effects of transverse stress and strength analysis of piezoelectric laminated structures. They report that electromechanical coupling effects of piezoelectric layers significantly increase the transverse stresses that can cause de-lamination and failure. Their primary goals were to produce interface and surface element and to impose the surface-traction-free condition on the continuity of the interlaminar transverse stress. An advantage of this type of analysis is that it produces elements that can adequately model thick piezoelectric laminated structures.

CHAPTER 2

Theory

2.1 Classical Lamination Theory

Important principles for analyzing thin plates were first introduced by Kirchhoff in the mid 1800s. Kirchhoff's hypothesis states,

(1) Straight lines perpendicular to the midsurface (i.e., transverse normals) before deformation remain straight after deformation.
(2) The transverse normals do not experience elongation (i.e., they are inextensible).
(3) The transverse normals rotate such that they remain perpendicular to the midsurface after deformation.

The first two assumptions imply that the transverse displacements are independent of the transverse coordinate and transverse normal strains are zero. The third implies zero transverse shear strain [Reddy, 1997]. The assumptions greatly simplify the analysis of laminated structures and have been verified experimentally by comparison with analysis of the same problem conducted without exploring the simplifying Kirchhoff hypothesis [Hyer, 1998].

Consider an *x-z* cross section of a laminated plate given in Figure 2.1a. It is assumed that all layers are perfectly bonded with no slippage, and the reference surface is taken as the geometric mid-plane. Line AA' passes through the laminate and is perpendicular to the reference surface.

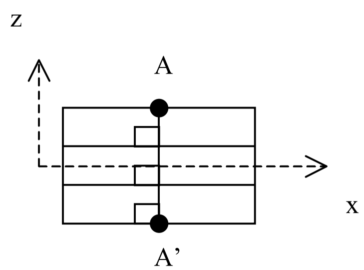

Figure 2.1a Undeformed

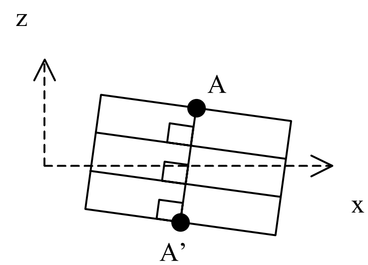

Figure 2.1b Deformed

Kirchhoff's hypothesis says that line AA' remain straight and normal to the deformed reference surface as seen in Figure 2.1b. It rotates and translates as a consequence of mid-plane deformations, but it does not deform. Because the deformations occur at the reference surface, the mechanics of the laminate can be expressed in terms of what happens at the reference surface.

Now, consider the same cross-section with reference plane deformations given in Figure 2.2. The displacement in the x-direction can be determined from the translation and rotation of point A, in the x-direction and about the y-axis, respectively.

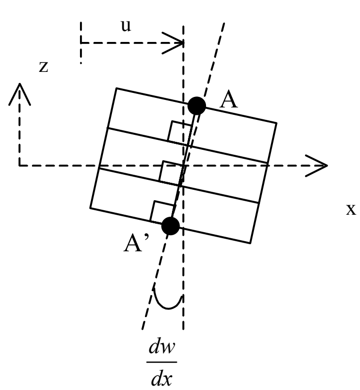

Figure 2.2 Kinematics of deformation as viewed in the x-z plane

In fact, the displacement of any point through the thickness of the laminate can be determined by

$$u(x,y,z) = u^o(x,y) - z\frac{\partial w^o(x,y)}{\partial x} \tag{2.1}$$

$$v(x,y,z) = v^o(x,y) - z\frac{\partial w^o(x,y)}{\partial y} \tag{2.2}$$

$$w(x,y,z) = w^o(x,y) \tag{2.3}$$

where u°, v°, and w° are the displacements at the reference surface.

If the displacement of the reference surface is known, the displacements, strains and stresses at each point along the normal line through the thickness can be determined, from equations (2.1), (2.2), and (2.3). The linear strains are determined from

$$\varepsilon_x(x,y,z) \equiv \frac{\partial u(x,y,z)}{\partial x} = \frac{\partial u^o(x,y)}{\partial x} - z\frac{\partial^2 w^o(x,y)}{\partial x^2} = \varepsilon_x^o + z\kappa_x^o \tag{2.4}$$

$$\varepsilon_y(x,y,z) \equiv \frac{\partial v(x,y,z)}{\partial y} = \frac{\partial v^o(x,y)}{\partial y} - z\frac{\partial^2 w^o(x,y)}{\partial y^2} = \varepsilon_y^o + z\kappa_y^o \tag{2.5}$$

$$\varepsilon_z(x,y,z) \equiv \frac{\partial w(x,y,z)}{\partial x} = \frac{\partial w^o(x,y)}{\partial z} = 0 \tag{2.6}$$

$$\gamma_{xy}(x,y,z) \equiv \frac{\partial v(x,y,z)}{\partial x} + \frac{\partial u(x,y,z)}{\partial y} = \gamma_{xy}^o + z\kappa_{xy}^o \tag{2.7}$$

$$\gamma_{xz}(x,y,z) \equiv \frac{\partial w(x,y,z)}{\partial x} + \frac{\partial u(x,y,z)}{\partial z} = 0 \tag{2.8}$$

$$\gamma_{yz}(x,y,z) \equiv \frac{\partial w(x,y,z)}{\partial y} + \frac{\partial v(x,y,z)}{\partial z} = 0 \tag{2.9}$$

The strain components through the thickness of the laminate are zero, based on Kirchhoff's hypothesis, and the resultant strains are

$$\varepsilon_x(x,y,z) = \varepsilon_x^o(x,y) + z\kappa_x^o(x,y) \tag{2.10}$$

$$\varepsilon_y(x,y,z) = \varepsilon_y^o(x,y) + z\kappa_y^o(x,y) \tag{2.11}$$

$$\gamma_{xy}(x,y,z) = \gamma_{xy}^o(x,y) + z\kappa_{xy}^o(x,y) \tag{2.12}$$

where

$$\begin{aligned}
\varepsilon_x^o(x,y) &= \frac{\partial u^o(x,y)}{\partial x} \quad and \quad \kappa_x^o(x,y) = -\frac{\partial^2 w^o(x,y)}{\partial x^2} \\
\varepsilon_y^o(x,y) &= \frac{\partial v^o(x,y)}{\partial y} \quad and \quad \kappa_x^o(x,y) = -\frac{\partial^2 w^o(x,y)}{\partial x^2} \\
\gamma_{xy}^o(x,y) &= \frac{\partial u^o(x,y)}{\partial y} + \frac{\partial v^o(x,y)}{\partial x} \quad and \quad \kappa_{xy}^o(x,y) = -2\frac{\partial^2 w^o(x,y)}{\partial x \partial y}
\end{aligned} \tag{2.13}$$

The quantities $\varepsilon_x^o, \varepsilon_y^o, \kappa_x^o, \kappa_y^o, \gamma_{xy}^o$, and κ_{xy}^o are the reference surface extensional strains, the reference surface curvatures, the reference surface in-plane shear strains, and the reference surface twisting curvatures, respectively.

Applying stress-strain relations (Hooke's Law), the strains can be defined in terms of the compliance matrix, *S*, and the stresses within the laminate are

$$\begin{bmatrix} \varepsilon_x \\ \varepsilon_y \\ \gamma_{xy} \end{bmatrix} = \begin{bmatrix} S_{11} & S_{12} & 0 \\ S_{21} & S_{22} & 0 \\ 0 & 0 & S_{33} \end{bmatrix} \begin{bmatrix} \sigma_x \\ \sigma_y \\ \tau_{xy} \end{bmatrix} \tag{2.14}$$

where

$$S_{11} = \frac{1}{E_1},\ S_{22} = \frac{1}{E_2},\ S_{12} = S_{21} = \frac{-\nu_{12}}{E_1} = \frac{-\nu_{21}}{E_2},\ S_{33} = \frac{1}{G_{12}} \tag{2.15}$$

The inverse of the compliance matrix is the called the reduce stiffness matrix, in which the stresses are written in term of the strains as

$$\begin{bmatrix} \sigma_x \\ \sigma_y \\ \tau_{xy} \end{bmatrix} = \begin{bmatrix} Q_{11} & Q_{12} & 0 \\ Q_{21} & Q_{22} & 0 \\ 0 & 0 & Q_{33} \end{bmatrix} \begin{bmatrix} \varepsilon_x \\ \varepsilon_y \\ \gamma_{xy} \end{bmatrix} \tag{2.16}$$

where

$$Q_{11} = \frac{S_{22}}{S_{11}S_{22} - S_{12}^2} \quad Q_{22} = \frac{S_{11}}{S_{11}S_{22} - S_{12}^2} \quad Q_{12} = Q_{21} = -\frac{S_{12}}{S_{11}S_{22} - S_{12}^2} \quad Q_{33} = \frac{1}{S_{33}} \tag{2.17}$$

Substituting the reference surface strains into equation (2.16) yields

$$\begin{bmatrix} \sigma_x \\ \sigma_y \\ \tau_{xy} \end{bmatrix} = \begin{bmatrix} Q_{11} & Q_{12} & 0 \\ Q_{21} & Q_{22} & 0 \\ 0 & 0 & Q_{33} \end{bmatrix} \begin{bmatrix} \varepsilon_x^o + z\kappa_x^o \\ \varepsilon_y^o + z\kappa_y^o \\ \gamma_{xy}^o + z\kappa_{xy}^o \end{bmatrix} \tag{2.18}$$

Based on the equation (2.18), the stresses are determined by the strains at the reference surface of the laminate. However, the stresses depend on z because material properties may vary from one layer to another. From this expression, the stresses and strains in each layer can be determined if the deformations of the reference surface are known.

2.1.1 Lamination Stiffness Matrix: The "*ABD*" Matrix

In the previous section, stress-strain relationships were derived based Kirchhoff's hypothesis. In this section, relationships between forces and moments applied at the reference surface are derived to determine equivalent stiffness matrices. Stress is defined as the force per unit cross-sectional area, and the moment is defined as the force times the distance from the reference surface. Using these relationships the forces and moments applied at the reference surface can be determined.

Consider a laminated plate given in figure 2.1.1.

Figure 2.3 Forces and moments applied to laminated plate

From the figure above the in-plane forces and moments per unit length, due to the stress, σ_x, are defined as

$$N_x = \int_{-h/2}^{h/2} \sigma_x \, dz \,, \quad M_x = \int_{-h/2}^{h/2} \sigma_x \; z \, dz \tag{2.19}$$

Substituting the expression in equations (2.18) into (2.19) yields

$$N_x = \int_{-h/2}^{h/2} \left\{ Q_{11}(\varepsilon_x^o + z\,\kappa_x^o) \; + \; Q_{12}(\varepsilon_y^o + z\,\kappa_y^o) \; + \; Q_{13}(\gamma_{xy}^o + z\,\kappa_{xy}^o) \right\} dz \tag{2.20}$$

$$\begin{aligned} N_x = & \left[\int_{-h/2}^{h/2} Q_{11} \; dz \right] \varepsilon_x^o + \left[\int_{-h/2}^{h/2} Q_{11} \; zdz \right] \kappa_x^o + \left[\int_{-h/2}^{h/2} Q_{12} \; dz \right] \varepsilon_y^o \\ & + \left[\int_{-h/2}^{h/2} Q_{12} \; z\,dz \right] \kappa_y^o + \left[\int_{-h/2}^{h/2} Q_{13} \; dz \right] \gamma_{xy}^o + \left[\int_{-h/2}^{h/2} Q_{13} \; z\,dz \right] \kappa_{xy}^o \end{aligned} \tag{2.21}$$

The first, third, and fifth terms (z^0 terms) in equation (2.21) are defined as

$$A_{ij} = \int_{-h/2}^{h/2} Q_{ij} \; dz \; = Q_{ij} \, h_k \tag{2.22}$$

for i=1, j=1,2,3

The term in the second, fourth, and sixth terms (z^1 terms) in equation (2.21) are defined as

$$B_{ij} = \int_{-h/2}^{h/2} Q_{ij}\ z\,dz = \frac{1}{2}\,Q_{ij}\,(h_k^2 - h_{k-1}^2) \tag{2.23}$$

for i=1, j=1,2,3

For multiple layers structures, equations (2.22) and (2.23) become

$$A_{ij} = \sum_{k=1}^{N} \int_{-h/2}^{h/2} Q_{ij}^k\ dz = \sum_{k=1}^{N} Q_{ij}^k\ h_k \tag{2.24}$$

$$B_{ij} = \sum_{k=1}^{N} \int_{-h/2}^{h/2} Q_{ij}^k\ z\ dz = \frac{1}{2} \sum_{k=1}^{N} Q_{ij}^k\ (h_k^2 - h_{k-1}^2) \tag{2.25}$$

for N=number of layers

By similar analysis, the strains at the reference surface are substituted for the stresses in the moment equation as follows:

$$M_x = \int_{-h/2}^{h/2} \left\{ Q_{11}(\varepsilon_x^o + z\,\kappa_x^o) + Q_{12}(\varepsilon_y^o + z\,\kappa_y^o) + Q_{13}(\gamma_{xy}^o + z\,\kappa_{xy}^o) \right\} z\,dz \tag{2.26}$$

$$\begin{aligned} M_x = {} & \left[\int_{-h/2}^{h/2} Q_{11}\ z dz\right]\varepsilon_x^o + \left[\int_{-h/2}^{h/2} Q_{11}\ z^2 dz\right]\kappa_x^o + \left[\int_{-h/2}^{h/2} Q_{12}\ z\,dz\right]\varepsilon_y^o \\ & + \left[\int_{-h/2}^{h/2} Q_{12}\ z^2\,dz\right]\kappa_y^o + \left[\int_{-h/2}^{h/2} Q_{13}\,z\,dz\right]\gamma_{xy}^o + \left[\int_{-h/2}^{h/2} Q_{13}\ z^2\,dz\right]\kappa_{xy}^o \end{aligned} \tag{2.27}$$

The first, third, and fifth terms (z^1 terms) in equation (2.27) are defined as

$$B_{ij} = \int_{-h/2}^{h/2} Q_{ij} \; z\, dz \; = \frac{1}{2}\, Q_{ij}\,(h_k^2 - h_{k-1}^2) \tag{2.28}$$

for i=1, j=1,2,3

The second, fourth, and sixth terms (z^2 terms) in equation (2.27) are defined as

$$D_{ij} = \int_{-h/2}^{h/2} Q_{ij} \; z^2\, dz \; = \frac{1}{3}\, Q_{ij}\,(h_k^3 - h_{k-1}^3) \tag{2.29}$$

for i=1, j=1,2,3

For multiple layers, equations (2.28) and (2.29) become

$$B_{ij} = \sum_{k=1}^{N} \int_{-h/2}^{h/2} Q_{ij}^k \; z \; dz \; = \frac{1}{2} \sum_{k=1}^{N} Q_{ij}^k \; (h_k^2 - h_{k-1}^2) \tag{2.30}$$

$$D_{ij} = \sum_{k=1}^{N} \int_{-h/2}^{h/2} Q_{ij}^k \; z^2 \; dz \; = \frac{1}{3} \sum_{k=1}^{N} Q_{ij}^k \; (h_k^3 - h_{k-1}^3) \tag{2.31}$$

The *A*, *B*, and *D* variables make up the laminate, *ABD*, stiffness matrix. With this definition, the reference surface loads are determined by the reference surface strains as

$$\begin{Bmatrix} N_x \\ N_y \\ N_{xy} \\ M_x \\ M_y \\ M_{xy} \end{Bmatrix} = \begin{bmatrix} A_{11} & A_{12} & A_{13} & B_{11} & B_{12} & B_{13} \\ A_{21} & A_{22} & A_{23} & B_{21} & B_{22} & B_{23} \\ A_{31} & A_{32} & A_{33} & B_{31} & B_{32} & B_{33} \\ B_{11} & B_{12} & B_{13} & D_{11} & D_{12} & D_{13} \\ B_{21} & B_{22} & B_{23} & D_{21} & D_{22} & D_{23} \\ B_{31} & B_{32} & B_{33} & D_{31} & D_{32} & D_{33} \end{bmatrix} \begin{Bmatrix} \varepsilon_x^o \\ \varepsilon_y^o \\ \gamma_{xy}^o \\ \kappa_x^o \\ \kappa_y^o \\ \kappa_{xy}^o \end{Bmatrix} \tag{2.32}$$

The *ABD* matrix defines a relationship between stress resultants (i.e., the loads) applied to a laminate and the reference surface strains and curvatures (i.e., the deformations). This form is the direct result of Kirchhoff hypothesis, plane stress assumptions, and the definition of stress resultants [Hyer, 1998].

To reiterate, for multiple layer structures the A, B, and D variables are defined by

$$A_{ij} = \sum_{k=1}^{N} \int_{-h/2}^{h/2} Q_{ij} \; dz \; = \sum_{k=1}^{N} Q_{ij} \, h_k \tag{2.33}$$

$$B_{ij} = \sum_{k=1}^{N} \int_{-h/2}^{h/2} Q_{ij} \; z \; dz \; = \frac{1}{2} \sum_{k=1}^{N} Q_{ij} \, (h_k^2 - h_{k-1}^2) \tag{2.34}$$

$$D_{ij} = \sum_{k=1}^{N} \int_{-h/2}^{h/2} Q_{ij} \; z^2 \; dz \; = \frac{1}{3} \sum_{k=1}^{N} Q_{ij} \, (h_k^3 - h_{k-1}^3) \tag{2.35}$$

for N=number of layers

Equation (2.32) can be written in a simplified form as follows:

$$\begin{Bmatrix} N \\ M \end{Bmatrix} = \begin{Bmatrix} A & B \\ B & D \end{Bmatrix} \begin{Bmatrix} \varepsilon^o \\ \kappa^o \end{Bmatrix} \tag{2.36}$$

2.2 Energy Methods and Classical Lamination Theory

In the previous section, classical lamination theory was applied to laminated structures. In this section, classical lamination theory will be integrated into energy methods to serve as a basis for solution techniques by the principle of minimum potential energy. In this section only the strain energy equations will be developed to incorporate techniques discussed in the previous sections for laminated structures.

2.2.1 Laminated Beams

Consider a cross section of a laminated beam as given in figure 2.2.1.

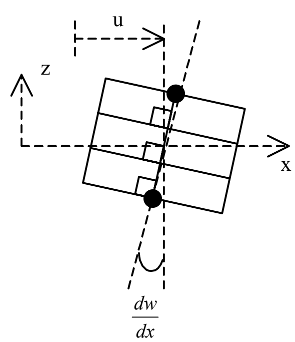

Figure 2.4 Cross-section of deformed laminated beam

From the previous section, the displacements were derived based on Kirchhoff's hypothesis and were given as

$$u(x,y,z) = u^o(x,y) - z\frac{\partial w^o(x,y)}{\partial x} \tag{2.37}$$

$$v(x,y,z) = v^o(x,y) - z\frac{\partial w^o(x,y)}{\partial y} \tag{2.38}$$

$$w(x,y,z) = w^o(x,y) \tag{2.39}$$

Here, Kirchhoff's hypothesis will still apply along with the plane strain assumptions. Applying plane strain, $\varepsilon_{yy}=\tau_{xy}=\tau_{yz}=0$, along with Kirchhoff's hypothesis, $\varepsilon_{zz}=\tau_{xz}=\tau_{yz}=0$. The only stress component, $\varepsilon_{xx,}$ will be

$$\varepsilon_{xx} = \frac{du}{dx} - z\frac{d^2 w}{dx^2} \tag{2.40}$$

The strain energy for each layer of the beam in figure (2.2.1) is given by

$$U_i = \frac{1}{2}\sum_{k=1}^{N}\iint_R \int_{-h/2}^{h/2} \sigma_{xx}^k \, \varepsilon_{xx} \, dz\, dx\, dy, \text{ where} \qquad \sigma_{xx}^k = E^k \varepsilon_{xx} \tag{2.41}$$

Since the strains in all three layers are equal (i.e., no slip plane), applying Hooke's law yields

$$U_i = \frac{1}{2}\sum_{k=1}^{N}\iint_R \int_{-h/2}^{h/2} E^k \varepsilon_{xx}^2 \; dz\, dx\, dy \tag{2.42}$$

Substituting the expression from strain in equation (2.38) into equation (2.40)

$$U_i = \frac{1}{2}\sum_{k=1}^{N}\iint_R \int_{-h/2}^{h/2} E^k \left(\frac{du}{dx} - z\frac{d^2 w}{dx^2}\right)^2 dz\, dx\, dy \tag{2.43}$$

Expanding equation (2.43) results in

$$U_i = \frac{1}{2}\sum_{k=1}^{N}\iint_R \int_{-h/2}^{h/2} E^k \left(\left(\frac{du}{dx}\right)^2 - 2z\frac{du}{dx}\frac{d^2 w}{dx^2} + \left(z\frac{d^2 w}{dx^2}\right)^2 \right) dz\, dx\, dy \tag{2.44}$$

Based on classical lamination theory, equation (2.42) can be simplified using *A*, *B*, *D* variables [Hyer, 1998], [Reddy,1997].

$$A_{ij} = \sum_{k=1}^{N} \int_{-h/2}^{h/2} Q_{ij}^{k} \; dz \; = \sum_{k=1}^{N} Q_{ij}^{k} \; h_k \tag{2.45}$$

$$B_{ij} = \sum_{k=1}^{N} \int_{-h/2}^{h/2} Q_{ij}^{k} \; z \; dz \; = \frac{1}{2} \sum_{k=1}^{N} Q_{ij}^{k} \; (h_k^2 - h_{k-1}^2) \tag{2.46}$$

$$D_{ij} = \sum_{k=1}^{N} \int_{-h/2}^{h/2} Q_{ij}^{k} \; z^2 \; dz \; = \frac{1}{3} \sum_{k=1}^{N} Q_{ij}^{k} \; (h_k^3 - h_{k-1}^3) \tag{2.47}$$

The variable Q_{ij} were defined previously as the reduced stiffness and are given as

$$Q_{11} = \frac{E_1}{1 - v_{12} v_{21}} \qquad Q_{22} = \frac{E_2}{1 - v_{12} v_{21}} \qquad Q_{12} = \frac{v_{12} E_1}{1 - v_{12} v_{21}} \qquad Q_{66} = G_{12} \tag{2.48}$$

With Kirchhoff's hypothesis and plane strain assumptions, the only strain component is ε_{xx}. Therefore, the equation for the strain energy is simplified as

$$U_{total} = \frac{1}{2} \iint_R \left[A_{11} \left(\frac{du}{dx} \right)^2 - 2B_{11} \frac{du}{dx} \frac{d^2 w}{dx^2} + D_{11} \left(\frac{d^2 w}{dx^2} \right)^2 \right] dx \, dy \tag{2.49}$$

The above expression represents strain energy of a laminated beam. For symmetric laminate, note that $B_{ij} = 0$ by the following expression:

$$\int_{-h/2}^{h/2} \left\{ 1, z, z^2 \right\} dz \; = \; \left\{ h, 0, \frac{h^3}{12} \right\} \tag{2.50}$$

Therefore equation (2.49) reduces to

$$U_{total} = \frac{1}{2} \iint_R \left[A_{11} \left(\frac{du}{dx} \right)^2 \quad + \; D_{11} \left(\frac{d^2 w}{dx^2} \right)^2 \right] dx\, dy \tag{2.51}$$

2.2.2 Laminated Plates

To extend the analysis to laminated plates, the plain strain assumption will no longer be valid. However, Kirchhoff's hypothesis will still apply, hence, $\varepsilon_{zz}=\tau_{xz}=\tau_{yz}=0$. The resultant strains will be given as

$$\begin{aligned} \varepsilon_{xx} &= \frac{du}{dx} - z\frac{d^2 w}{dx^2} \\ \varepsilon_{yy} &= \frac{dv}{dy} - z\frac{d^2 w}{dy^2} \\ \varepsilon_{xy} &= \left(\frac{du}{dy} + \frac{dv}{dx} \right) - 2\, z\, \frac{d^2 w}{dx\, dy} \end{aligned} \tag{2.52}$$

The strain energy for each layer of the plate is given as

$$U_i = \frac{1}{2} \sum_{k=1}^{N} \iint_R \int_{-h/2}^{h/2} \sigma^k \, \varepsilon \quad dz\, dx\, dy \tag{2.53}$$

By Hooke's law, the stresses are

$$\begin{bmatrix} \sigma_{xx} \\ \sigma_{yy} \\ \sigma_{xy} \end{bmatrix} = \begin{bmatrix} Q_{11} & Q_{12} & 0 \\ Q_{21} & Q_{22} & 0 \\ 0 & 0 & Q_{66} \end{bmatrix} \begin{bmatrix} \varepsilon_{xx} \\ \varepsilon_{yy} \\ \varepsilon_{xy} \end{bmatrix} \tag{2.54}$$

Substituting the expression for stress into equation (2.53) yields

$$U_i = \frac{1}{2}\sum_{k=1}^{N}\iint_R \int_{-h/2}^{h/2} \left[Q_{ij}^k \varepsilon_{xx}^2 + 2Q_{ij}^k \varepsilon_{xx}\varepsilon_{yy} + Q_{ij}^k \varepsilon_{yy}^2 + Q_{ij}^k \varepsilon_{xy}^2 \right] dz\, dx\, dy \tag{2.55}$$

The above expression in matrix form will be

$$U_i = \frac{1}{2}\sum_{k=1}^{N}\iint_R \int_{-h/2}^{h/2} \varepsilon^T Q^k \varepsilon \quad dz\, dx\, dy \tag{2.56}$$

Substituting the expression for strain in equation (2.52) into equation (2.55) results in

$$U_i = \frac{1}{2}\sum_{k=1}^{N}\iint_R \int_{-h/2}^{h/2} \left\{ \frac{du}{dx} - z\frac{d^2w}{dx^2} \quad \Big| \quad \frac{dv}{dy} - z\frac{d^2w}{dy^2} \quad \Big| \quad \left(\frac{du}{dy} + \frac{dv}{dx}\right) - 2z\frac{d^2w}{dxdy} \right\} \begin{bmatrix} Q_{11}^k & Q_{12}^k & 0 \\ Q_{21}^k & Q_{22}^k & 0 \\ 0 & 0 & Q_{33}^k \end{bmatrix} \begin{Bmatrix} \frac{du}{dx} - z\frac{d^2w}{dx^2} \\ \frac{dv}{dy} - z\frac{d^2w}{dy^2} \\ \left(\frac{du}{dy} + \frac{dv}{dx}\right) - 2z\frac{d^2w}{dxdy} \end{Bmatrix} dzdxdy$$

(2.57)

Equation (2.57) represents the strain energy for each layer of a laminated plate. The strain energy for a laminated plate, substituting the expressions for *ABD* given in equations (2.45), (2.46), and (2.47), is

$$U_{total} = \frac{1}{2}\iint_R \left\{ \frac{du}{dx} \;\middle|\; \frac{dv}{dy} \;\middle|\; \left(\frac{du}{dy} + \frac{dv}{dx}\right) \right\} \begin{bmatrix} A_{11} & A_{12} & 0 \\ A_{21} & A_{22} & 0 \\ 0 & 0 & A_{33} \end{bmatrix} \begin{Bmatrix} \frac{du}{dx} \\ \frac{dv}{dy} \\ \left(\frac{du}{dy} + \frac{dv}{dx}\right) \end{Bmatrix} -$$

$$\left\{ \frac{du}{dx} \;\middle|\; \frac{dv}{dy} \;\middle|\; \left(\frac{du}{dy} + \frac{dv}{dx}\right) \right\} \begin{bmatrix} B_{11} & B_{12} & 0 \\ B_{21} & B_{22} & 0 \\ 0 & 0 & B_{33} \end{bmatrix} \begin{Bmatrix} \frac{d^2w}{dx^2} \\ \frac{d^2w}{dy^2} \\ 2\frac{d^2w}{dx\,dy} \end{Bmatrix} + \qquad (2.58)$$

$$\left\{ \frac{d^2w}{dx^2} \;\middle|\; \frac{d^2w}{dy^2} \;\middle|\; 2\frac{d^2w}{dx\,dy} \right\} \begin{bmatrix} D_{11} & D_{12} & 0 \\ D_{21} & D_{22} & 0 \\ 0 & 0 & D_{33} \end{bmatrix} \begin{Bmatrix} \frac{d^2w}{dx^2} \\ \frac{d^2w}{dy^2} \\ 2\frac{d^2w}{dx\,dy} \end{Bmatrix} dx\,dy$$

The above expression represents the total strain energy for a laminated plate, where the first terms represent the strain energy due to stretching, the intermediate terms represent the stretching and bending coupling effects, and the last terms represent the strain energy due to bending.

The intermediate terms in equation (2.58) are zero for symmetric laminates; therefore, the equation reduces to

$$U_{total} = \frac{1}{2}\iint_R \left\{ \frac{du}{dx} \quad \middle| \quad \frac{dv}{dy} \quad \middle| \quad \frac{du}{dy} + \frac{dv}{dx} \right\} \begin{bmatrix} A_{11} & A_{12} & 0 \\ A_{21} & A_{22} & 0 \\ 0 & 0 & A_{33} \end{bmatrix} \begin{Bmatrix} \frac{du}{dx} \\ \frac{dv}{dy} \\ \frac{du}{dy} + \frac{dv}{dx} \end{Bmatrix} \quad +$$

$$\left\{ \frac{d^2 w}{dx^2} \quad \middle| \quad \frac{d^2 w}{dy^2} \quad \middle| \quad 2\frac{d^2 w}{dx\, dy} \right\} \begin{bmatrix} D_{11} & D_{12} & 0 \\ D_{21} & D_{22} & 0 \\ 0 & 0 & D_{33} \end{bmatrix} \begin{Bmatrix} \frac{d^2 w}{dx^2} \\ \frac{d^2 w}{dy^2} \\ 2\frac{d^2 w}{dx\, dy} \end{Bmatrix} \; dx\, dy \qquad (2.59)$$

The derivations of strain energy in this section will serve as a basis for solution techniques by the principle of minimum potential energy.

2.3 Linear Theory of Piezoelectricity

The equations of piezoelectricity have been around since the days of Voigt. However, most of the literature on piezoelectricity was written from different practical viewpoints. One of the earliest authors to systematically model the electromechanical coupling effects of piezoelectric materials was Tiersten [1969]. The constitutive equations for piezoelectricity are derived from the internal strain energy, electric fields, and electric displacements. The internal energy is given by

$$U = \frac{1}{2} S T + \frac{1}{2} D E \tag{2.60}$$

$$U = \frac{1}{2} c_{ijkl} S_{ij} S_{kl} + \frac{1}{2} \varepsilon_{ij} E_i E_j \tag{2.61}$$

where

$S_{ij} = \frac{1}{2}(u_{i,j} + u_{j,i})$	mechanical strain
$E_k = -\varphi_{,k}$	electric field
φ	electric potential
ε_{ij}	dielectric constants
c_{ijkl}	elastic constants
s_{ijkl}	inverse elastic constants
$e_{ijk} = s_{ijkl}\, d_{ijk}$	piezoelectric stress coefficients
$d_{ijk} = c_{ijkl}\, d_{ijk}$	piezoelectric strain coefficients

The constitutive equations of piezoelectricity are derived from the electric enthalpy, which is defined as

$$H = U - E_i D_i \tag{2.62}$$

$$H = \frac{1}{2} c_{ijkl} S_{ij} S_{kl} - e_{ijk} E_i S_{jk} - \frac{1}{2} \varepsilon_{ij} E_i E_j \tag{2.63}$$

Differentiating the enthalpy with respect to the strain, *S*, and electric field, *E*, defines the constitutive equations of piezoelectricity. The equations are

$$\tau_{ij} = \frac{\partial H}{\partial S_{ij}} \tag{2.64}$$

$$D_i = -\frac{\partial H}{\partial E_i} \tag{2.65}$$

$$\tau_{ij} = c_{ijkl} S_{kl} - e_{ijk} E_k \qquad \text{piezoelectric stress} \tag{2.66}$$

$$D_i = e_{ikl} S_{kl} - \varepsilon_{ik} E_k \qquad \text{electric displacement} \tag{2.67}$$

The equations of motion will be derived by Hamilton's principles for the piezoelectric medium. The Lagrangian equation for the bounded piezoelectric medium is defined as

$$L = \int_V (T + V)\, dV \tag{2.68}$$

where T is the kinetic energy and V is the potential energy.

For the electromechanical medium, the electric enthalpy takes the place of the internal energy in the Lagrangian density [Tiersten, 1969]. The potential energy is therefore given as

$$V = -\int_V \left[\frac{1}{2} c_{ijkl} S_{ij} S_{kl} - e_{ijk} E_i S_{jk} - \frac{1}{2} \varepsilon_{ij} E_i E_j \right] dV \tag{2.69}$$

The kinetic energy is defined as the mass per unit volume (density) and is given as

$$T = \int_V \left[\frac{1}{2} \rho \dot{u}_j \dot{u}_j \right] dV \tag{2.70}$$

The external work terms are defined as the work done by surface tractions less the flux of electric energy outward across the surface and is given as

$$W = \int_S \left[t\, u_j - \bar{\sigma} \varphi \right] dS \tag{2.71}$$

$t - surface\ tractions,\ \bar{\sigma} - surface\ charge$

Applying Hamilton's principle results in the following:

$$\delta(L - W) = 0 \ , \quad \delta L = \delta W \tag{2.72}$$

$$\delta \int_V \left[\frac{1}{2} \rho \dot{u}_j \dot{u}_j - \frac{1}{2} c_{ijkl} S_{ij} S_{kl} + e_{ijk} E_i S_{jk} + \frac{1}{2} \varepsilon_{ij} E_i E_j \right] dV = \delta \int_S \left[t\, u_j - \bar{\sigma} \varphi \right] dS \tag{2.73}$$

The variation with respect to the displacements and electrical potentials results in the following:

$$\int_V \left(\rho \dot{u}_j \dot{u}_j - \tau_{kl,k} \right) \delta u_l \ dV - \int_V D_{k,k} \, \delta \varphi \, dV = \int_S \left[(t_k - n_k \tau_{kl}) \delta u - (\sigma + \bar{n}_k D_k) \, \delta \varphi \right] dS \tag{2.74}$$

In the equation (2.73), the variations in the displacements are arbitrary inside the volume; hence, we define the stress equations of motion as

$$\rho \dot{u}_j \dot{u}_j - \tau_{kl,k} = 0 \tag{2.75}$$

Also, the variations in the potential are arbitrary inside the volume; hence, we define the charge equation of electrostatics as

$$D_{k,k} = 0 \tag{2.76}$$

From equation (2.74) on the surface,

-Since δu_l is arbitrary, either $t_l - n_k \tau_{kl} = 0$ or u_l is prescribed.

-Since $\delta \varphi$ is arbitrary either $\sigma + n_k D_k = 0$ or φ is prescribed.

Using variational principles, the differential equations and the boundary conditions for the piezoelectric medium have been defined.

CHAPTER 3

Analytical Modeling

3.1 Finite Element Analysis

Finite element method is a powerful computational technique for solutions of differential and integral equations [Reddy,1997]. Exact analytical or variational solutions are difficult to develop when complex geometries, arbitrary boundary conditions, or nonlinearities are involved. Therefore, finite element methods are used to represent the domain as an assemblage of simple geometric shapes for which it is possible to generate approximation functions required in differential equations of variational methods [Reddy, 1997].

Finite element methods are very similar to Rayleigh-Ritz techniques. Although, developed independently, the methods both make use of approximation functions and variational methods to approximate solutions to differential equations. The major difference in the two methods is that finite element methods uses approximations functions over a small subdomain of the structure, whereas Rayleigh-Ritz techniques uses approximation functions over the entire domain of the structure. The approximation functions are practical only if the geometric boundary conditions are satisfied.

The static equilibrium equations for beams/plates are derived using the principle of minimum potential energy and variational calculus. Finite element analysis requires discretization of the domain such that solutions are approximated over a small subdomain, which are assembled to obtain the global system representing the structure. Upon imposition of boundary conditions, the solutions to the system of equations are obtainable.

3.1.1 Interpolation Functions:

The purpose of interpolation functions is to relate the element degrees of freedom to the displacement field. Beams/plates exhibit C^0 continuity in stretching (i.e., axial deformation), and C^1 continuity in bending (i.e., transverse deformation). C^0 continuity requires that only the displacements be continuous at the element boundaries, while C^1 continuity requires that the displacements and the slopes be continuous at the element boundaries.

3.1.2 Interpolation Functions for Beams in Stretching

Assuming a linear solution across the element subdomain derives the interpolation functions for C^o elements. The governing equation for beams in stretching is given as

$$\frac{\partial^2 u}{\partial x^2} = 0 \tag{3.1}$$

where u is the axial displacement. The solution to the governing equation is approximated as

$$u(x) = c_1 + c_2 x = \begin{bmatrix} 1 & x \end{bmatrix} \begin{bmatrix} c_1 \\ c_2 \end{bmatrix} \tag{3.2}$$

Consider a two-node beam, given in figure 3.1.

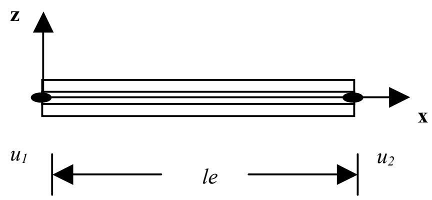

Figure 3.1 A laminated beam element

Imposition of the boundary conditions in equation (3.2) and solving for c_1 and c_2 results in

$$\begin{bmatrix} u_1 \\ u_2 \end{bmatrix} = \begin{bmatrix} 1 & 0 \\ 1 & le \end{bmatrix} \begin{bmatrix} c_1 \\ c_2 \end{bmatrix} \text{ , hence } \begin{bmatrix} c_1 \\ c_2 \end{bmatrix} = \begin{bmatrix} 1 & 0 \\ -\frac{1}{le} & \frac{1}{le} \end{bmatrix} \begin{bmatrix} u_1 \\ u_2 \end{bmatrix} \tag{3.3}$$

Substituting the constants into the linear approximations given in equation (3.2) yields

$$u(x) = \begin{bmatrix} 1 & x \end{bmatrix} \begin{bmatrix} 1 & 0 \\ -\frac{1}{le} & \frac{1}{le} \end{bmatrix} \begin{bmatrix} u_1 \\ u_2 \end{bmatrix} \tag{3.4}$$

The interpolations functions are extracted and the approximation function is given in the following form

$$u(x) = u_1^e \psi_1^e + u_2^e \psi_2^e = \sum_{j=1}^{2} u_j^e \psi_j^e \tag{3.5}$$

where u_1 and u_2 are the displacement at the boundaries of the beam.

Therefore the interpolation functions from equation (3.4) for the element are given as

$$\{\psi_1, \psi_2\} = \begin{bmatrix} 1 & x \end{bmatrix} \begin{bmatrix} 1 & 0 \\ -\frac{1}{le} & \frac{1}{le} \end{bmatrix} = \left\{ 1 - \frac{x}{le}, \ \frac{x}{le} \right\} \tag{3.6}$$

$$\psi_1 = 1 - \frac{x}{le} \ , \ \psi_2 = \frac{x}{le} \\ N_a = \{\psi_1 \ , \psi_2\} \tag{3.7}$$

3.1.3 Interpolation Functions for Beams in Bending

The interpolation functions for beam in bending are derived similar to the previous interpolation functions; however, the elements now exhibit C^1 continuity. The governing equation for beams in bending is

$$\frac{\partial^4 w}{\partial x^4} = 0 \tag{3.8}$$

where w is the transverse displacement. The solution to equation (3.8) is approximated as

$$w(x) = c_1 + c_2 \ x + c_3 \ x^2 + c_4 \ x^3 \tag{3.9}$$

To extract the interpolation functions, the approximation will be given the following form:

$$w(x) = w_1\,\phi_1 + w_2\,\phi_2 + w_3\,\phi_3 + w_4\,\phi_4 = \sum_{j=1}^{4} w_j\,\phi_j \tag{3.10}$$

where w_1 and w_3 are the transverse displacements and w_2 and w_4 are slopes at the boundaries. Imposition of the boundary conditions and solving for the four constants, the interpolations functions will be

$$\begin{aligned} &\phi_1 = 1 - 3\left(\frac{x}{l_e}\right)^2 + 2\left(\frac{x}{l_e}\right)^3 \;,\quad \phi_2 = -x\left(1 - \frac{x}{l_e}\right)^2 \;, \\ &\phi_3 = 3\left(\frac{x}{l_e}\right)^2 - 2\left(\frac{x}{l_e}\right)^3 \;,\quad \phi_4 = -x\left[\left(\frac{x}{l_e}\right)^2 - \frac{x}{l_e}\right] \\ &N_t = \{\phi_1\,,\,\phi_2\,,\,\phi_3\,,\,\phi_4\} \end{aligned} \tag{3.11}$$

3.1.4 Energy Methods and Lamination Theory

From the previous sections, the strain energy for a symmetrically laminated beam in bending was given as

$$U_{total} = \frac{1}{2}\iint_R \left[A_{11}\left(\frac{du}{dx}\right)^2 - 2B_{11}\frac{du}{dx}\frac{d^2w}{dx^2} + D_{11}\left(\frac{d^2w}{dx^2}\right)^2\right] dx\,dy \tag{3.12}$$

Applying the principle of minimum potential energy, such that

$$\delta(U - W) = 0 \;,\quad \delta U = \delta W \tag{3.13}$$

where W is the work done on the structure, minimizes the functional.

Taking the first variation of the strain energy with respect to the axial and transverse displacements result in

$$\delta U_{total} = \iint_R \begin{bmatrix} \left[A_{ij}\left(\frac{d\psi_j^e}{dx}\frac{d\psi_i^e}{dx}\right)u_i \; - B_{ij}\left(\frac{d\psi_j^e}{dx}\frac{d^2\phi_i^e}{dx^2}\right)w_i \right]\delta u_i \\ -\left[B_{ij}\left(\frac{d^2\phi_j^e}{dx^2}\frac{d\psi_i^e}{dx}\right)u_i \; + D_{ij}\left(\frac{d^2\phi_j^e}{dx^2}\frac{d^2\phi_i^e}{dx^2}\right)\right]\delta w_i \end{bmatrix} dxdy \tag{3.14}$$

From the above expression, the element stiffness matrices are defined as

$$\begin{aligned} K_{11}^e &= \iint_R A_{ij}\left(\frac{d\psi_j^e}{dx}\frac{d\psi_i^e}{dx}\right) dx\, dy \\ K_{12}^e &= -\iint_R B_{ij}\left(\frac{d\psi_j^e}{dx}\frac{d^2\phi_i^e}{dx^2}\right) dx\, dy \\ K_{21}^e &= -\iint_R B_{ij}\left(\frac{d^2\phi_j^e}{dx^2}\frac{d\psi_i^e}{dx}\right) dx\, dy \\ K_{22}^e &= \iint_R D_{ij}\left(\frac{d^2\phi_j^e}{dx^2}\frac{d^2\phi_i^e}{dx^2}\right) dx\, dy \end{aligned} \tag{3.15}$$

The work done by external loads is

$$W_{total} = \iint_R \left[t\left(u - z\frac{dw}{dx}\right) + f_t w \right] dx\, dy + \iint_R \left[f_a u\right] dy\, dz \tag{3.16}$$

where t are traction forces across the surface, f_t are transverse forces, and f_a are axial forces.

Taking the first variation with respect to the axial and transverse displacements, the virtual work done on the beam will be given as

$$\delta W_{total} = \iint_R \left[\psi_j\, t\right]\delta u_i\, dx\, dy + \iint_R \left[\psi_j f_a\right]\delta u_i\; dy\, dz + \iint_R \left[\phi_j\, f_t - z\frac{d\phi_j}{dx}t\right]\delta w_i\, dx\, dy \tag{3.17}$$

The element force vectors will, therefore, be defined as

$$F_1^e = \iint_R \left[\psi_j t\right] dx\, dy \ + \iint_R \left[\psi_j f_a\right] dy\, dz$$
$$F_2^e = \iint_R \left[\phi_j\ f_t - z\ \frac{d\phi_j}{dx} t\ \right] dx\, dy \tag{3.18}$$

Applying the principle of minimum potential energy, equation (3.13), the static equilibrium equations are defined as

$$\begin{bmatrix} K_{11}^e & K_{12}^e \\ K_{21}^e & K_{22}^e \end{bmatrix} \begin{Bmatrix} u \\ w \end{Bmatrix} = \begin{Bmatrix} F_1^e \\ F_2^e \end{Bmatrix} \tag{3.19}$$

3.2 Finite Element Analysis for Piezoelectric Beams

The finite element formulations for piezoelectric beams are similar to the formulations for elastic beams. However, since the material is piezoelectric, the beam will have axial, transverse, rotational, and electrical degrees of freedom at the nodal locations. The derivations are not found in many textbooks, but they are based on classical beam theory, the linear theory of piezoelectricity, energy methods and variational principles.

3.2.1 Interpolation Functions

The interpolation functions for the axial, transverse, and rotational degrees of freedom are the same as for elastic beams in equations (3.7) and (3.11)

The electrical degrees of freedom for piezoelectric materials are given by the electric potential, and the electric field, as defined previously, is the gradient of the electrical potential. Consider the piezoelectric beam given in Figure 3.2.

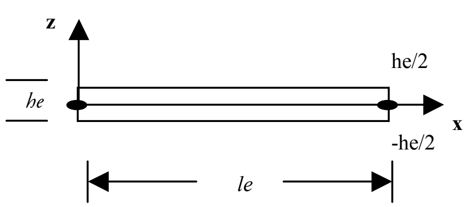

Figure 3.1 A laminated beam element

The governing equation for the electric potentials is

$$-\nabla^2 \varphi = 0 \tag{3.20}$$

Approximating the solution to equation (3.20) results in

$$\varphi(z) = c_1 + c_2 z = \begin{bmatrix} 1 & z \end{bmatrix} \begin{bmatrix} c_1 \\ c_2 \end{bmatrix} \tag{3.21}$$

To extract the interpolation functions, the approximation function will be given the following form

$$\varphi(z) = \varphi_1 \xi_1 + \varphi_2 \xi_2 = \sum_{j=1}^{2} \varphi_j \xi_j \tag{3.22}$$

where φ_1 and φ_2 are the electric potentials at the top and bottom surface of the beam.

The electric potentials at the boundary are arbitrary, unless specified [Tiersten, 1969], and may vary along the length of the beam; hence, they will be functions of the thickness and length of the beam.

Upon imposition of the boundary conditions and solving for the unknown constants the interpolation functions through the thickness of the beam are

$$\begin{gathered} \xi^*_{1_1} = \frac{1}{2} + \frac{z}{he} \,, \quad \xi^*_{2_2} = \frac{1}{2} - \frac{z}{he} \\ N_{e_e}^* = \left\{ \xi^*_1 \,, \xi^*_{2_2} \right\} \end{gathered} \tag{3.23}$$

The interpolation function will also be a function of the length of the beam, therefore, the product of the axial and through the thickness interpolation functions relate the electrical degrees of freedom to the nodes and is given as

$$N_e = N_a \, N_e^* = \left\{ 1 - \frac{x}{le} \;,\quad \frac{x}{le} \right\} \left\{ \frac{1}{2} + \frac{z}{he} \;,\; \frac{1}{2} - \frac{z}{he} \right\} \tag{3.24}$$

Homogenous boundary conditions for the electric potentials will be imposed on the bottom surface to eliminate rigid body modes. Therefore, the interpolation functions are

$$\begin{aligned} N_e &= N_a \, N_e^* = \left\{ 1 - \frac{x}{le} \;,\quad \frac{x}{le} \right\} \left\{ \frac{1}{2} + \frac{z}{he} \right\} \\ \xi_1 &= \left(\frac{1}{2} + \frac{z}{he} \right) \left(1 - \frac{x}{le} \right), \; \xi_2 = \left(\frac{1}{2} + \frac{z}{he} \right) \left(\frac{x}{le} \right) \\ N_e &= \{ \xi_1 \;, \xi_2 \} \end{aligned} \tag{3.25}$$

3.2.2 Energy Methods and Variational Principles

Finite element formulations for piezoelectric beams are derived similar to the derivations for elastic beams. The electric enthalpy for a piezoelectric medium is defined as

$$H = U \, - \, E_i \, D_i \tag{3.26}$$

$$H = \frac{1}{2} c_{ijkl} S_{ij} S_{kl} \, - \, e_{ijk} E_i S_{jk} \, - \, \frac{1}{2} \varepsilon_{ij} \, E_i \, E_j \tag{3.27}$$

For electromechanical medium, the electric enthalpy takes the place of the internal energy in the Lagrangian density [Tiersten, 1969]. Therefore, the potential energy is given by

$$V = -\int_V \left[\frac{1}{2} c_{ijkl} S_{ij} S_{kl} \, - \, e_{ijk} E_i S_{jk} \, - \, \frac{1}{2} \varepsilon_{ij} \, E_i \, E_j \right] dV \tag{3.28}$$

Consider the piezoelectric beam given in Figure 3.2, applying plane stress and plane strain assumptions, the displacement field and strains are

$$u(x,y,z)=u(x)-z\frac{\partial w(x)}{\partial x} \tag{3.29}$$

$$S_{ij}=\frac{\partial u}{\partial x}-z\frac{\partial^2 w}{\partial x^2} \tag{3.30}$$

The electric field is defined as the gradient of the electric potential, which is given as

$$E_i=-\varphi_{k,k}=-\frac{\partial \varphi}{\partial z} \tag{3.31}$$

Upon substitution of the stress and electric field into equation (3.28) yield

$$V=-\int_V\left[\frac{1}{2}c_{ijkl}\left(\frac{\partial u}{\partial x}-z\frac{\partial^2 w}{\partial x^2}\right)^2-e_{ijk}\left(-\frac{\partial \varphi}{\partial z}\right)\left(\frac{\partial u}{\partial x}-z\frac{\partial^2 w}{\partial x^2}\right)-\frac{1}{2}\varepsilon_{ij}\left(-\frac{\partial \varphi}{\partial z}\right)^2\right]dV \tag{3.32}$$

The approximation functions were previously defined as

$$u(x)=\sum_{i=1}^{2}\psi_i\,u_i \tag{3.33}$$

$$w(x)=\sum_{i=1}^{4}\phi_i\,w_i \tag{3.34}$$

$$\varphi(x,z)=\sum_{i=1}^{2}\xi_i\varphi_i \tag{3.35}$$

To minimize the potential energy, the first variation is evaluated with respect to the axial and transverse displacements, and the electric potentials.

Upon taking the variation, and substituting the approximation functions into equation (3.32) yields

$$\delta V = \int_V \left[c_{ijkl}\left(\frac{\partial \psi_j}{\partial x}\frac{\partial \psi_i}{\partial x}\right)u_i - c_{ijkl}z\left(\frac{\partial \psi_j}{\partial x}\frac{\partial^2 \phi_i}{\partial x^2}\right)w_i + e_{ijk}\left(\frac{\partial \psi_j}{\partial x}\frac{\partial \xi_i}{\partial z}\right)\varphi_i\right]\delta u_i \, dV -$$
$$\int_V \left[c_{ijkl}\, z\left(\frac{\partial^2 \phi_j}{\partial x^2}\frac{\partial \psi_i}{\partial x}\right)u_i - c_{ijkl}z^2\left(\frac{\partial^2 \phi_j}{\partial x^2}\frac{\partial^2 \phi_i}{\partial x^2}\right)w_i + e_{ijk}\, z\left(\frac{\partial^2 \phi_j}{\partial x^2}\frac{\partial \xi_i}{\partial z}\right)\varphi_i\right]\delta w_i \, dV +$$
$$\int_V \left[c_{ijkl}\left(\frac{\partial \xi_j}{\partial z}\frac{\partial \psi_i}{\partial x}\right)u_i - c_{ijkl}z\left(\frac{\partial \xi_j}{\partial z}\frac{\partial^2 \phi_i}{\partial x^2}\right)w_i - \varepsilon_{ij}\left(\frac{\partial \xi_j}{\partial z}\frac{\partial \xi_i}{\partial z}\right)\varphi_i\right]\delta \varphi_i \, dV \tag{3.36}$$

Applying methods from classical lamination theory (i.e., *ABD*), where *c* represents the reduced stiffness, *Q*, the element stiffness is

$$K_{11}^e = \iint_R A_{ij}\left(\frac{d\psi_j^e}{dx}\frac{d\psi_i^e}{dx}\right)dx\,dy$$
$$K_{12}^e = -\iint_R B_{ij}\left(\frac{d\psi_j^e}{dx}\frac{d^2\phi_i^e}{dx^2}\right)dx\,dy$$
$$K_{13}^e = \iint_R\int e_{ijk}\left(\frac{d\psi_j^e}{dx}\frac{d\,\xi_i^e}{dz}\right)dx\,dy\,dz$$
$$K_{21}^e = -\iint_R B_{ij}\left(\frac{d^2\phi_j^e}{dx^2}\frac{d\psi_i^e}{dx}\right)dx\,dy$$
$$K_{22}^e = \iint_R D_{ij}\left(\frac{d^2\phi_j^e}{dx^2}\frac{d^2\phi_i^e}{dx^2}\right)dx\,dy$$
$$K_{23}^e = -\iint_R\int e_{ijk}\,z\left(\frac{d^2\phi_j^e}{dx^2}\frac{d\,\xi_i^e}{dz}\right)dx\,dy\,dz$$
$$K_{31}^e = \iint_R\int e_{ijk}\left(\frac{d\,\xi_j^e}{dz}\frac{d\psi_i^e}{dx}\right)dx\,dy\,dz$$
$$K_{32}^e = -\iint_R\int e_{ijk}\,z\left(\frac{d\,\xi_j^e}{dz}\frac{d^2\phi_i^e}{dx^2}\right)dx\,dy\,dz \tag{3.37}$$
$$K_{33}^e = -\iint_R\int \varepsilon_{ij}\left(\frac{d\,\xi_j^e}{dz}\frac{d\,\xi_i^e}{dz}\right)dx\,dy\,dz$$

The work done by external loads is defined as

$$W_{total} = \iint_R \left[t\left(u - z\frac{dw}{dx} \right) + f_t w - \sigma\varphi \right] dx\, dy + \iint_R \left[f_a u \right] dy\, dz \tag{3.38}$$

where t are traction forces across the surface, f_t are transverse forces, f_a are axial forces, and σ are the surface charges.

The first variation of the virtual work, after substitution of the approximation functions, is

$$\begin{aligned} \delta W_{total} = &\iint_R \left[\psi_j\, t \right] \delta u_i\, dx\, dy + \iint_R \left[\psi_j f_a \right] \delta u_i\; dy\, dz - \\ &\iint_R \left[\xi_j\, \sigma \right] \delta \varphi_i\, dx\, dy + \iint_R \left[\phi_j\, f_t - z\frac{d\phi_j}{dx} t \right] \delta w_i\, dx\, dy \end{aligned} \tag{3.39}$$

The element load vectors will, therefore, be given as

$$\begin{aligned} F_1^e &= \iint_R \left[\psi_j t \right] dx\, dy + \iint_R \left[\psi_j f_a \right] dy\, dz \\ F_2^e &= \iint_R \left[\phi_j\, f_t - z\, \frac{d\phi_j}{dx} t \right] dx\, dy \\ F_3^e &= -\iint_R \left[\xi_j \sigma \right] dx\, dy \end{aligned} \tag{3.40}$$

The equilibrium equations are now obtainable by the principle of minimum potential energy as

$$\begin{bmatrix} K_{11}^e & K_{12}^e & K_{13}^e \\ K_{21}^e & K_{22}^e & K_{23}^e \\ K_{31}^e & K_{32}^e & K_{33}^e \end{bmatrix} \begin{Bmatrix} u \\ w \\ \varphi \end{Bmatrix} = \begin{Bmatrix} F_1^e \\ F_2^e \\ F_3^e \end{Bmatrix} \tag{3.41}$$

3.3 Equivalent Electromechanical Loading Techniques

Much research has been conducted on modeling the electromechanical effects of laminated piezoelectric structures [1, 3, 6, 9, 12, 16, 30, 31, 41]. Many authors have developed finite element methods for modeling piezoelectric structures [3, 5, 10, 12, 30, 31, 34], and many software packages support piezoelectric modeling to some extent. However, ABAQUS does not support piezoelectric elements for dynamic analysis, and only continuum and one dimensional truss elements are supported for piezoelectric static modeling.

In this section, we introduce equivalent mechanical loading techniques for modeling piezoelectric materials subjected to electrical actuating forces. Two methods will be introduced to serve as equivalent loading techniques for modeling piezoelectric structures. The first method will be developed based on matrix manipulations and techniques similar to "static condensation," which has been introduced in a number of publications [10,31]. A second technique will be developed based on a engineering mechanics and the linear theory of piezoelectricity.

3.3.1 Equivalent Loading and Static Condensation

Many recent publications have introduced matrix manipulation techniques for deriving equivalent mechanical models to capture the electromechanical coupling effects of piezoelectric materials. These models can very well serve as equivalent mechanical models of coupled electromechanical systems. However, they do not distinctly represent an equivalent uncoupled purely elastic system. The motivation for developing such a model is to determine equivalent effects, due to electrical and mechanical loading. Several authors conduct what is called "static condensation of the electric potentials," in which equations are manipulated such that electric potentials are written in terms of the material properties and electrical loads.

The static equilibrium equations are

$$\begin{bmatrix} K_{mm} & K_{m\varphi} \\ K_{\varphi m} & K_{\varphi\varphi} \end{bmatrix}\begin{bmatrix} u_m \\ u_\varphi \end{bmatrix}=\begin{bmatrix} F_m \\ F_\varphi \end{bmatrix} \tag{3.42}$$

The electric potential are then written in terms of the stiffness matrices, mechanical displacement, and electrical loads vectors as

$$\left[u_\varphi\right]=\left[K_{\varphi\varphi}^{-1}\left(F_\varphi - K_{\varphi m}\, u_m\right)\right] \tag{3.43}$$

The expression in equation (3.43) is substituted in to the equilibrium equations and the equivalent mechanical system is given as

$$\left[K_{mm} - K_{m\varphi}\, K_{\varphi\varphi}^{-1}\left(K_{\varphi m}\right)\right]\left[u_m\right]= \left[F_m - K_{\varphi\varphi}^{-1}\, F_\varphi\right] \tag{3.44}$$

An equivalent system is derived from equation (3.44) but the system is still coupled. This leads to the derivation of an equivalent uncoupled system.

Equation (3.42) is rewritten in term of the displacements and electric potentials, which yield

$$\begin{bmatrix} u_m \\ u_\varphi \end{bmatrix}=\begin{bmatrix} K_{mm} & K_{m\varphi} \\ K_{\varphi m} & K_{\varphi\varphi} \end{bmatrix}^{-1}\begin{bmatrix} F_m \\ F_\varphi \end{bmatrix} \tag{3.45}$$

For simplicity, we will let

$$\begin{bmatrix} K_{mm} & K_{m\varphi} \\ K_{\varphi m} & K_{\varphi\varphi} \end{bmatrix}^{-1} = \begin{bmatrix} K^{*}_{mm} & K^{*}_{m\varphi} \\ K^{*}_{\varphi m} & K^{*}_{\varphi\varphi} \end{bmatrix} \tag{3.46}$$

such that

$$\begin{bmatrix} u_{m} \\ u_{\varphi} \end{bmatrix} = \begin{bmatrix} K^{*}_{mm} & K^{*}_{m\varphi} \\ K^{*}_{\varphi m} & K^{*}_{\varphi\varphi} \end{bmatrix} \begin{bmatrix} F_{m} \\ F_{\varphi} \end{bmatrix} \tag{3.47}$$

Now the assumption is that the loading condition is purely electrical; hence the mechanical loads are zero. This allows us to solve for the mechanical displacements in terms of the stiffness and electric loads, which results in

$$[u_{m}] = \left[K^{*}_{m\varphi}\right]\left[F_{\varphi}\right] \tag{3.48}$$

Now that we know the mechanical displacements for any given electrical load, we can substitute the expression into a purely elastic model and determine an equivalent mechanical load as

$$\begin{aligned} [F_{m}] &= [K_{mm}][u_{m}] \\ [F_{m}] &= [K_{mm}]\left[K^{*}_{m\varphi}\right]\left[F_{\varphi}\right] \end{aligned} \tag{3.49}$$

From equation (3.49), the mechanical force vector can be used to determine the equivalent mechanical displacements of a purely elastic model. The advantage of this method is that we can model the static response of an electromechanically coupled system using a purely elastic representation.

3.3.2 Constitutive Equations of Piezoelectricity

The second method of developing equivalent representations of electromechanical-coupled systems is based on the linear theory of piezoelectricity. The constitutive equation for a piezoelectric beam is given as

$$\sigma = cS - eE \tag{3.50}$$

where S is the strain, c is modulus of elasticity, e is the piezoelectric stress coefficient, and E is the electric field. The beam subjected to a distributed surface charge will induce a strain without causing a stress within the material, as depicted in Figure 3.3.

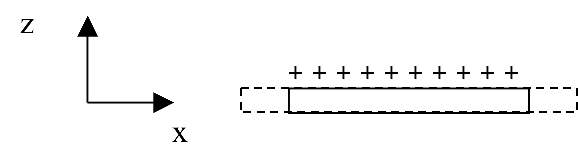

Figure 3.3 Surface charge applied to piezoelectric beam element

To determine the axial loads, required to restore the beam to its original configuration, the beam is blocked at both ends as shown in Figure 3.4.

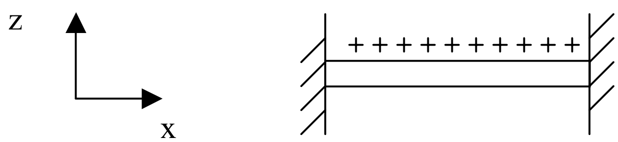

Figure 3.4 Blocked piezoelectric beam with applied electrical loading

The electrical surface charge now induces a stress within the material without resulting in any strain, so constitutive equation reduces to

$$\sigma_x = -e_{31} E_3 \tag{3.51}$$

Replacing the stress in equation (3.51) with force per unit area results in

$$\frac{F_b}{A_{zy}} = -e_{31} E_3 \tag{3.52}$$

The force generated within the material is termed the "blocking force," and the area is the cross sectional area of the beam. Solving equation (3.52), the blocking force is

$$F_b = -e_{31} E_3 A_{zy} \tag{3.53}$$

The relationship between charge and electric field for two parallel plates with a dielectric material occupying the space between is

$$E = \frac{Q}{\kappa_o A_{xy}} \tag{3.54}$$

where k_o is the dielectric constant and A_{xy} is the surface area of the plate. Substitution of the above expression into equation (3.53) yields

$$F_b = -\left(\frac{A_{zy}\, e_{31}}{\kappa_o A_{xy}}\right) Q \qquad (3.55)$$

The blocking force given in equation (3.55) represents the equivalent loading condition for the piezoelectric beam.

A surface-mounted piezoelectric material produces both axial forces and moments, the latter being a function of the distance the piezoelectric layer and the geometric mid-plane. For a symmetric bimorph configuration, the axial loads cancel resulting in only equivalent moments about the geometric mid-plane.

CHAPTER 4

Quantifications with ABAQUS Results

4.1 Multiple Layer vs. Single Layer Modeling

Multiple layer structures can be model as a single layer with equivalent material properties based on classical lamination theory. In this section, classical lamination theories were quantified by comparisons of multiple layers versus equivalent single layer modeling. The purpose of the analysis was to compare the static response of the modeling to determine the error in the assumptions made by Kirchhoff and to validate modeling multiple layer structures with single layer equivalent structures.

The analysis began with three models of a beam subject to identical boundary and loading conditions. One of the models was composed of two layers of polyvinylidene fluoride (PVDF) in a bimorph configuration and a single layer of shape memory alloy (SMA), Nitinol. The other models were single layer models of equivalent material properties. The laminated structure was developed using ABAQUS. The element types used for modeling the piezoelectric layers of the laminated structure were twenty-node, three-dimensional continuum piezoelectric elements (C3D20RE); for the shape memory alloy layer, twenty-node, three-dimensional continuum elements (C3D20R) were used. An equivalent model was developed in ABAQUS using two dimensional beam elements (B23) with equivalent material properties based on classical lamination theory. A similar model was also developed in Matlab using beam elements of equivalent material properties that were derived based on beam theory, the principle of minimum potential energy, and classical lamination theory. The beam models were all generated using twenty elements for comparison of the nodal displacements. The geometric and material properties of the models are given in the following tables:

Table 4.1 Geometric properties of a piezoelectric laminated beam

Length	10 cm
Width	1 cm
PVDF thickness	0.05 cm (x2)
SMA thickness	0.05 cm
Total thickness	0.15 cm

Table 4.2 Material properties of a piezoelectric laminated beam

PVDF Elastic Modulus: (E)	2 GPa
Piezoelectric stress coefficient: (e_{31})	-0.14 C/m^2
Dielectric constant: ($\in_{33}/\in_0$)	11.98
SMA Elastic Modulus (E)	6.95 GPa

Table 4.3 Equivalent geometric and material properties for a piezoelectric laminated beam

PVDF/SMA/PVDF Elastic Modulus: (E)	2.183 GPa
Piezoelectric stress coefficient: (e_{31})	-0.14 C/m^2
Dielectric constant: ($\in_{33}/\in_0$)	11.98

A simply supported beam was subjected to a distributed mechanical load of 1 N/m is shown in Figure 4.1.

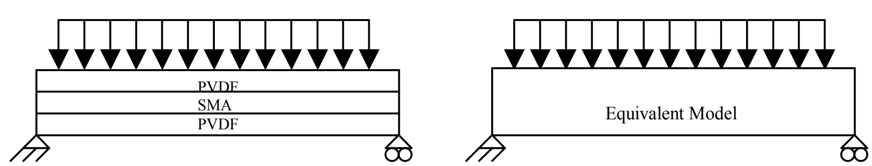

Figure 4.1 Multiple and single layer structure with applied distributed loads

An overlay of the solutions for the multiple layer and single layer equivalent beam models is shown in Figure 4.2,

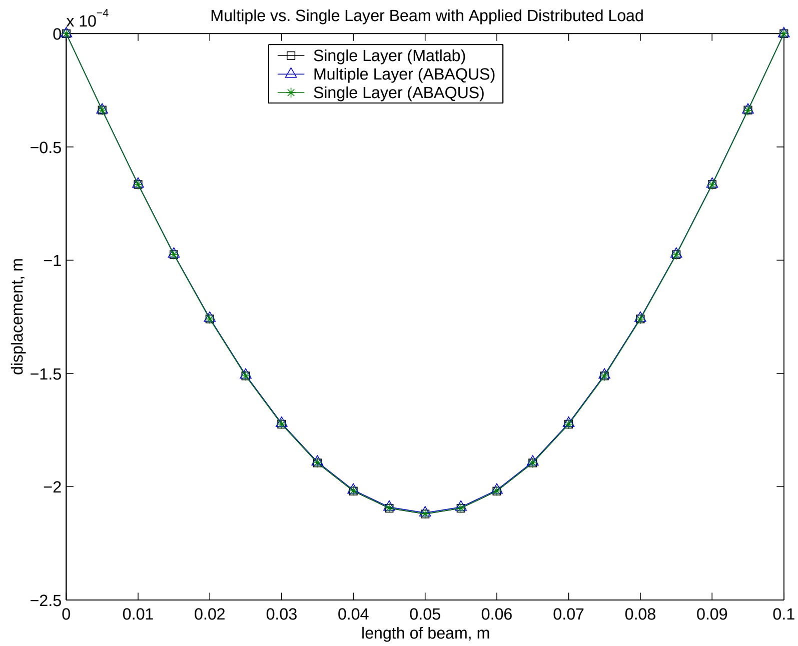

Figure 4.2 Comparisons of multiple and single layer modeling

The solutions for the multiple layer and single layer modeling coincide to the third decimal digit, with a difference of much less than 1%.

A second test case was conducted on the beam with the distributed load applied over a small patch, as shown schematically in figure 4.3.

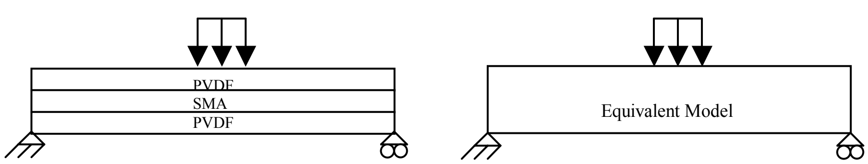

Figure 4.3 Multiple and single layer structure with applied distributed loads over a small patch

Numerical comparisons of the multiple layer modeling and single layer models are given in the following table, and an overlay of the displaced shapes shown in Figure 4.4.

Table 4.4 Numerical comparisons for multiple and single layer modeling

x (m)	w(x)		
	Multiple Layer ABAQUS x1e-1 (mm)	Single Layer ABAQUS x1e-1 (mm)	Single Layer MATLAB x1e-1 (mm)
0	0	0	0
0.0050	-0.0506	-0.0504	-0.0506
0.0100	-0.1001	-0.0999	-0.1001
0.0150	-0.1476	-0.1473	-0.1476
0.0200	-0.1920	-0.1916	-0.1920
0.0250	-0.2324	-0.2319	-0.2324
0.0300	-0.2676	-0.2671	-0.2677
0.0350	-0.2967	-0.2961	-0.2969
0.0400	-0.3187	-0.3181	-0.3189
0.0450	-0.3326	-0.3319	-0.3328
0.0500	-0.3374	-0.3366	-0.3376
0.0550	-0.3326	-0.3319	-0.3328
0.0600	-0.3188	-0.3181	-0.3189
0.0650	-0.2968	-0.2961	-0.2969
0.0700	-0.2676	-0.2671	-0.2677
0.0750	-0.2324	-0.2319	-0.2324
0.0800	-0.1921	-0.1916	-0.1920
0.0850	-0.1477	-0.1473	-0.1476
0.0900	-0.1002	-0.0999	-0.1001
0.0950	-0.0507	-0.0504	-0.0506
0.1000	0	0	0

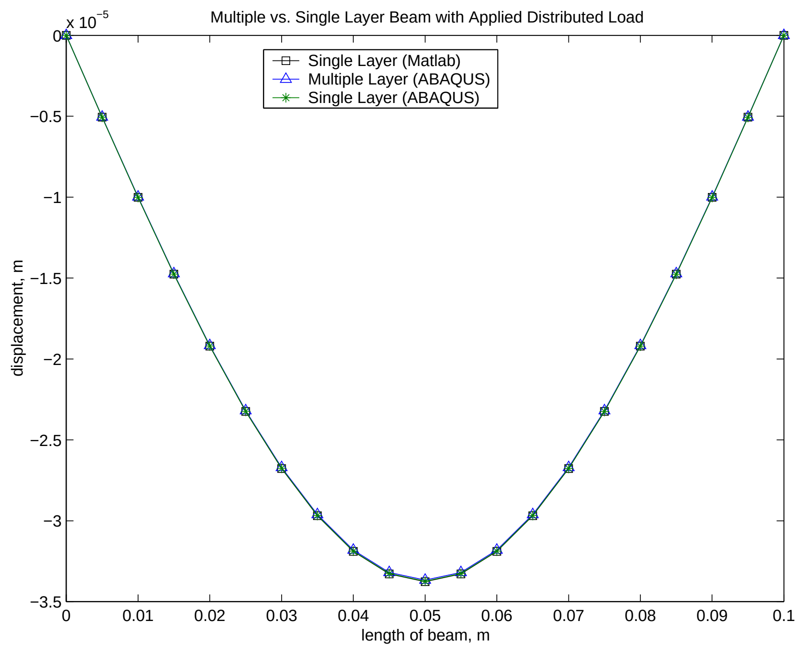

Figure 4.4 Comparisons of multiple and single layer modeling

From the results given in the analysis, it is concluded that Kirchhoff's assumptions are valid and classical lamination theory serves as an accurate modeling technique for simplifying the analysis of multiple layer structures.

4.2 Piezoelectric Modeling

Finite element methods were developed for piezoelectric beams based on the linear theory of piezoelectricity. The piezoelectric elements derived include axial, transverse, rotational, and electrical degrees of freedom. The purpose of deriving such an element was to capture the mechanical and electrical characteristics of the piezoelectric structure. In this section, finite element formulations were tested by comparison to models generated using ABAQUS. The purpose of the analysis was to compare theoretical results to ABAQUS results and to analyze the errors made in the assumptions used to generate mathematical models.

The analysis began with two finite element models of a piezoelectric beam subject to identical boundary and electrical loading conditions. One of the models was generated using the piezoelectric modeling capabilities of ABAQUS, with twenty-node, three-dimensional continuum piezoelectric elements (C3D20RE). The other model was generated in Matlab, based on beam theory, the principle of minimum potential energy and the linear theory of piezoelectricity. Both beam models were generated using twenty elements for comparisons of the nodal displacements. The material properties of the structures are given in the following tables.

Table 4.5 Geometric properties for a piezoelectric beam

Length	10 cm
Width	1 cm
PVDF thickness	0.15 cm
Total thickness	0.15 cm

Table 4.6 Material properties for a piezoelectric beam

PVDF Elastic Modulus: (E)	2 GPa
Piezoelectric stress coefficient: (e_{31})	-0.14 C/m^2
Dielectric constant: ($\in_{33}/\in_0$)	11.98

A simply supported beam was subjected to a distributed electrical load of 1e6 C/m, as shown in Figure 4.5 an overlay of the ABAQUS and Matlab results are shown in Figure 4.6.

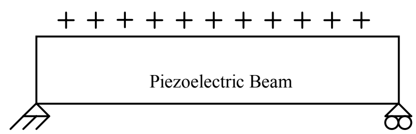

Figure 4.5 Distributed electrical load applied to a piezoelectric beam

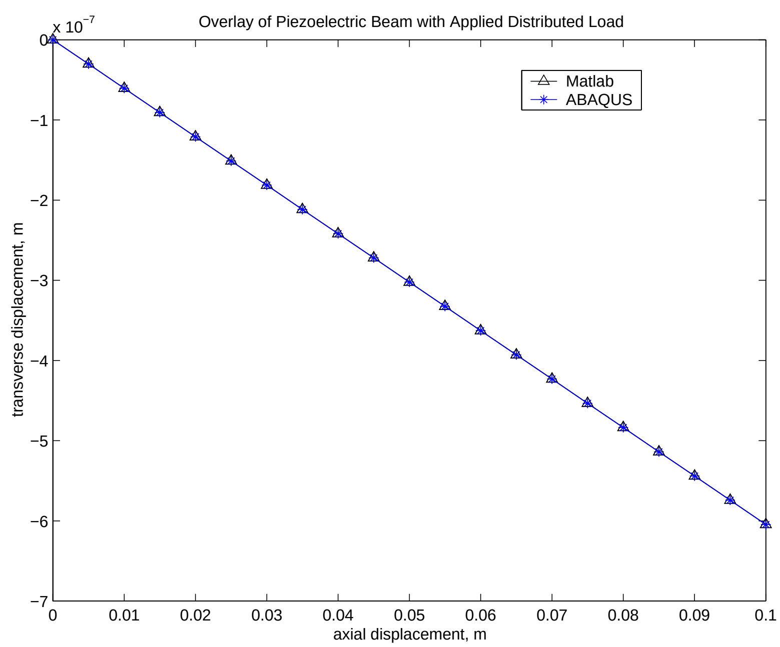

Figure 4.6 Comparisons of Matlab and ABAQUS results for piezoelectric beam modeling

Numerical comparisons of the two models are given in the following table,

Table 4.7 Numerical comparisons for Matlab and ABAQUS models

Node Location	Axial Displacements u(x)	
	ABAQUS results	MATLAB results
1	0	0
2	-0.0302	-0.0302
3	-0.0604	-0.0604
4	-0.0907	-0.0907
5	-0.1209	-0.1209
6	-0.1511	-0.1511
7	-0.1814	-0.1813
8	-0.2116	-0.2116
9	-0.2418	-0.2418
10	-0.2720	-0.2720
11	-0.3023	-0.3022
12	-0.3325	-0.3325
13	-0.3627	-0.3627
14	-0.3929	-0.3929
15	-0.4231	-0.4231
16	-0.4534	-0.4534
17	-0.4836	-0.4836
18	-0.5138	-0.5138
19	-0.5440	-0.5440
20	-0.5743	-0.5743
21	-0.6045	-0.6045

Based on the results given in Table 4.7, the computational and theoretical solutions agree to four decimal digits, a difference much less than 1%.

4.3 Piezoelectric Laminated Modeling

The analysis of piezoelectric beams in the previous section resulted in excellent agreement between theoretical and ABAQUS solutions. In this section, classical lamination theory was applied to modeling piezoelectric laminated structures. Results generated in ABAQUS were compared with results from theoretical models based on beam theory, classical lamination theory, the principle of minimum potential energy, and the linear theory of piezoelectricity. The purpose of the analysis was to simplify the analysis of piezoelectric laminated structures.

The analysis began with two finite element models of a piezoelectric beam subject to identical boundary and electrical loading conditions. One of the models was composed of two layers of polyvinylidene fluoride (PVDF) in a bimorph configuration and one layer of shape memory alloy (SMA), Nitinol. The piezoelectric layers of the laminated model were generated using the piezoelectric capabilities of ABAQUS. The elements used for the PVDF layers were twenty-node, three-dimensional continuum piezoelectric elements (C3D20RE); the elements used for the SMA layer were twenty node, three-dimensional continuum elements (C3D20R). The theoretical model was generated in Matlab, based on beam theory, classical lamination theory, the principle of minimum potential energy, and the linear theory of piezoelectricity. Both beam models were generated using twenty elements for comparisons of the nodal displacements. The material and geometric properties of the beams are given in the following tables.

Table 4.8 Geometric properties of a piezoelectric laminated beam:

Length	10 cm
Width	1 cm
PVDF thickness	0.05 cm (x2)
SMA thickness	0.05 cm
Total thickness	0.15 cm

Table 4.9 Material properties of a piezoelectric laminated beam

PVDF Elastic Modulus: (E)	2 GPa
Piezoelectric stress coefficient: (e_{31})	-0.14 C/m^2
Dielectric constant: ($\in_{33}/\in_0$)	11.98
SMA Elastic Modulus (E)	6.95 GPa

A simply supported beam was subjected to a distributed electrical load of 1e6 C/m, as shown in Figure 4.7.

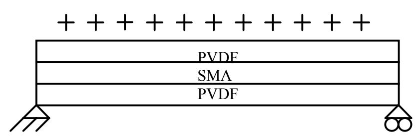

Figure 4.7 Distributed electrical load applied to a piezoelectric laminated beam

A laminated structure generated in ABAQUS was compared to Matlab solutions. Overlays of the results are shown in the following figure.

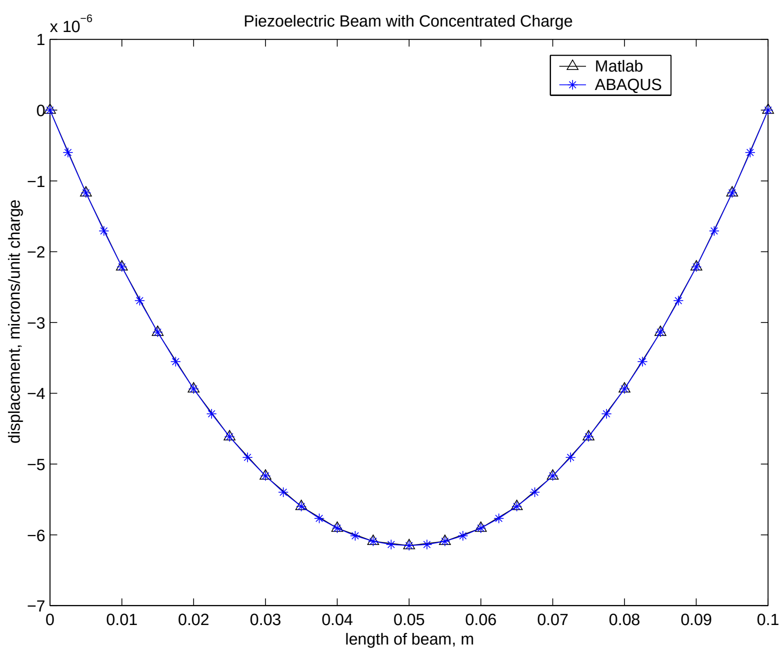

Figure 4.8 Comparisons of Matlab and ABAQUS results for laminated piezoelectric beam modeling

The Matlab and ABAQUS results in figure (4.8) coincide to three decimal digits. The difference in the two solutions was much less than 1%.

A second analysis of the laminated structure was conducted to determine the response due to distributed loads applied over an element. A schematic is shown in Figure 4.9, and an overlay of the results is shown in Figure 4.10.

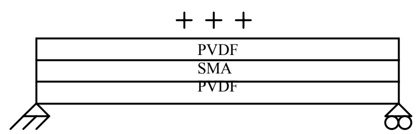

Figure 4.9 Distributed electrical load applied over a small patch of a laminated piezoelectric beam

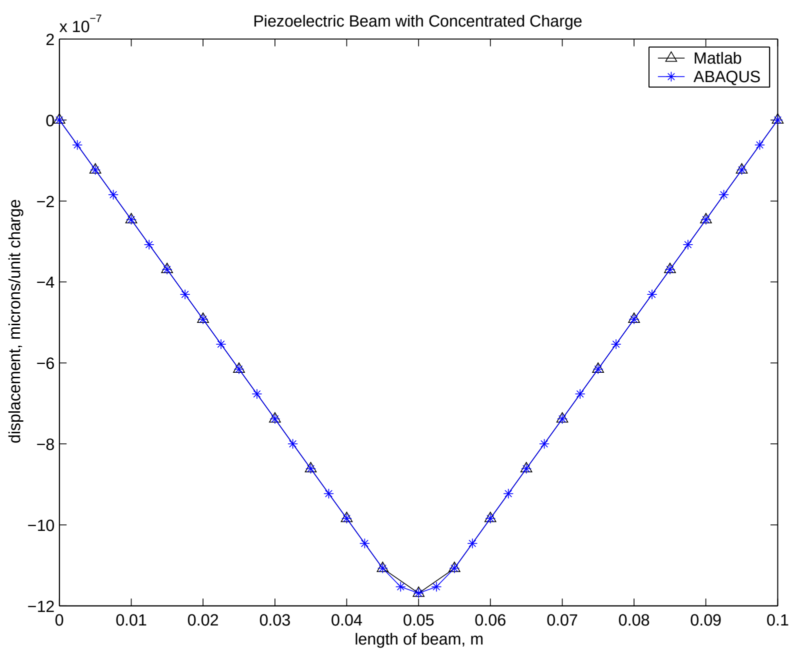

Figure 4.10 Comparisons of Matlab and ABAQUS results for laminated piezoelectric beam modeling

The numerical results are given in the Table 4.10.

Table 4.10 Numerical comparisons for Matlab and ABAQUS models

x (m)	w(x) ABAQUS x1e-2 (mm)	w(x) MATLAB x1e-2 (mm)
0	0	0
0.0050	-0.0123	-0.0123
0.0100	-0.0246	-0.0246
0.0150	-0.0369	-0.0369
0.0200	-0.0492	-0.0492
0.0250	-0.0615	-0.0615
0.0300	-0.0738	-0.0738
0.0350	-0.0861	-0.0861
0.0400	-0.0984	-0.0984
0.0450	-0.1107	-0.1107
0.0500	-0.1169	-0.1169
0.0550	-0.1107	-0.1107
0.0600	-0.0984	-0.0984
0.0650	-0.0861	-0.0861
0.0700	-0.0738	-0.0738
0.0750	-0.0615	-0.0615
0.0800	-0.0492	-0.0492
0.0850	-0.0369	-0.0369
0.0900	-0.0246	-0.0246
0.0950	-0.0123	-0.0123
0.1000	0.0000	0

Based on the numerical results given in Table 4.10, the Matlab and ABAQUS results agree to four decimal digits, a difference less than 1%. From the analysis in this section, theoretical models (Matlab) produce very accurate approximations.

4.4 Equivalent Loading vs. Deposition of Surface Charges

Equivalent electromechanical loading techniques were derived, in the previous chapter, to simulate electrical surface charge actuations of piezoelectric materials. In this section, the equivalent loading techniques were quantified by comparisons with ABAQUS models of laminated structures subjected to electrical loading conditions. The purpose of the analysis in this section was to simplify the analysis of piezoelectric laminated structures subjected to electrical loads. The goal was to model an equivalent structure with equivalent material properties that capture the electrical and mechanical characteristics of the structure.

The analysis began with two models of a beam subject to identical boundary and loading conditions. One of the models was a laminated structure composed of two layers of polyvinylidene fluoride (PVDF) in a bimorph configuration and a single layer of shape memory alloy (SMA), Nitinol. The piezoelectric modeling capabilities of ABAQUS were used to model the piezoelectric layers. The piezoelectric layers were modeled using twenty-node, three-dimensional continuum piezoelectric elements (C3D20RE); and the shape memory alloy layer was modeled using twenty-node, three dimension continuum elements (C3D20R). The equivalent model was generated in ABAQUS using two dimensional beam elements (B23) with equivalent material properties of the laminated structure. Both models were generated with twenty elements for comparisons of the nodal displacements. The geometric and material properties of the beam are given in the following table.

Table 4.11 Geometric properties of a piezoelectric laminated beam

Length	10 cm
Width	1 cm
PVDF thickness	0.05 cm (x2)
SMA thickness	0.05 cm
Total thickness	0.15 cm

Table 4.12 Material properties of a piezoelectric laminated beam

PVDF Elastic Modulus: (E)	2 GPa
Piezoelectric stress coefficient: (e_{31})	-0.14 C/m^2
Dielectric constant: ($\in_{33}/\in_0$)	11.98
SMA Elastic Modulus (E)	6.95 GPa

Table 4.13 Material properties for equivalent beam model

PVDF/SMA/PVDF Elastic Modulus: (E)	2.183 GPa
Piezoelectric stress coefficient: (e_{31})	-0.14 C/m^2
Dielectric constant: ($\in_{33}/\in_0$)	11.98

A simply supported beam subjected to a distributed electrical surface charge of 1e6 C/m, and the equivalent model with equivalent electromechanical loading conditions are shown in Figure 4.11.

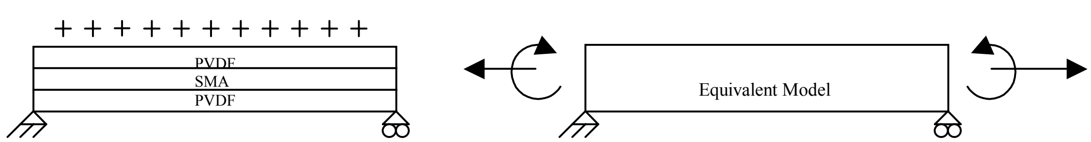

Figure 4.11 Piezoelectric laminated beam with distributed electrical loading and equivalent beam with equivalent loading

The equivalent mechanical loading conditions were calculated based on methods discussed in the previous chapter. Two methods for determining the loading conditions were discussed, and both methods produced identical solutions.

An overlay of the results using the equivalent loading techniques versus the piezoelectric laminated model is shown in Figure 4.12.

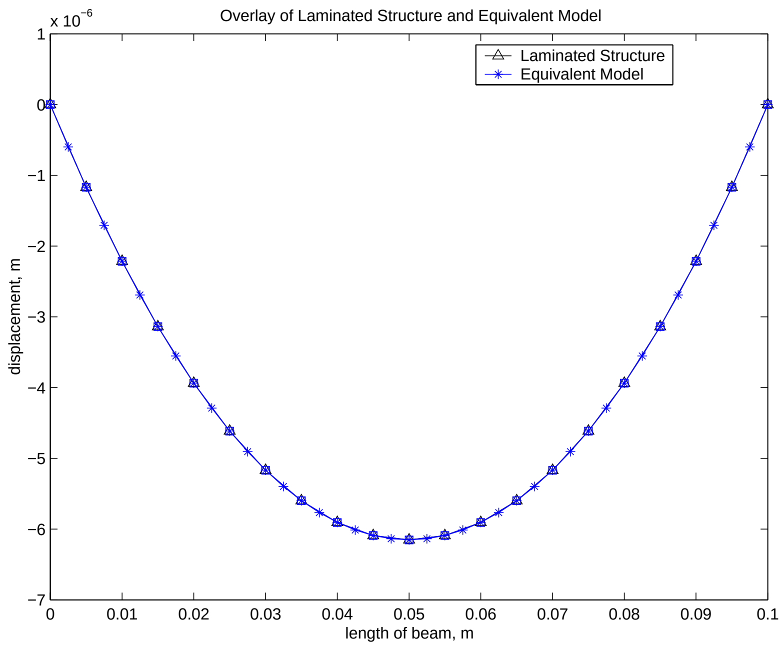

Figure 4.12 Comparison of laminated piezoelectric beam and equivalent model

A second analysis was conducted to compare the response of the beam when subjected to a distributed load over a small patch, shown schematically in Figure 4.13.

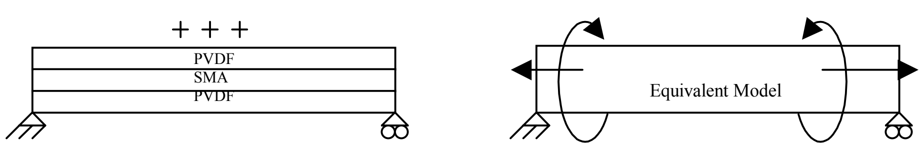

Figure 4.13 Piezoelectric laminated beam with electrical loading and equivalent beam with equivalent loading

Equivalent moment and axial forces calculated in the previous chapter were applied to simulate the surface charge shown in Figure 4.13.

The numerical results from the analysis are shown in Table 4.14, and an overlay of the solutions is shown in Figure 4.14.

Table 4.14 Numerical comparisons for laminated piezoelectric modeling and equivalent modeling

x (m)	w(x)		
	ABAQUS Electrical Loading x1e-2 (mm)	MATLAB Electrical Loading x1e-2 (mm)	ABAQUS Equivalent Loading x1e-2 (mm)
0	0	0	0
0.0050	-0.0123	-0.0123	-0.0123
0.0100	-0.0246	-0.0246	-0.0246
0.0150	-0.0369	-0.0369	-0.0369
0.0200	-0.0492	-0.0492	-0.0492
0.0250	-0.0615	-0.0615	-0.0615
0.0300	-0.0738	-0.0738	-0.0738
0.0350	-0.0861	-0.0861	-0.0861
0.0400	-0.0984	-0.0984	-0.0984
0.0450	-0.1107	-0.1107	-0.1107
0.0500	-0.1169	-0.1169	-0.1168
0.0550	-0.1107	-0.1107	-0.1107
0.0600	-0.0984	-0.0984	-0.0984
0.0650	-0.0861	-0.0861	-0.0861
0.0700	-0.0738	-0.0738	-0.0738
0.0750	-0.0615	-0.0615	-0.0615
0.0800	-0.0492	-0.0492	-0.0492
0.0850	-0.0369	-0.0369	-0.0369
0.0900	-0.0246	-0.0246	-0.0246
0.0950	-0.0123	-0.0123	-0.0123
0.1000	0.0000	0	0

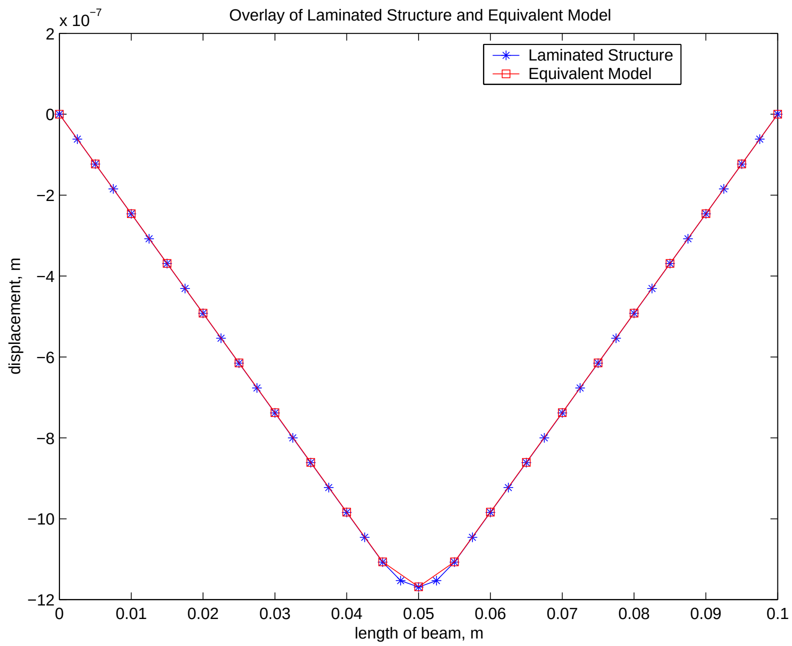

Figure 4.14 Comparisons of laminated piezoelectric beam and equivalent model

The results given in Table 4.14, show that the two approaches agree within 1%.

From the analysis in this section, modeling laminated piezoelectric structures with electrical loading conditions have been greatly simplified with equivalent models with equivalent loading conditions. Equivalent models of laminated piezoelectric beams and plates can now be accomplished, and deriving theoretical models, based on classical lamination theory, beam/plate theory, the principle of minimum potential energy, and the linear theory of piezoelectricity, has validated them.

4.5 Plate Modeling

Finally, the analysis was extended to plates. Finite element models were developed for equivalent single layer plate, piezoelectric plate, piezoelectric laminated plates, and equivalent plate with equivalent loading techniques. Classical lamination theory of plates was used to derive mathematical solutions for the laminated plate. The plate theory is very similar to beam theory, only now, the plane strain theory is no longer valid. Plate analysis, therefore, involves two additional degrees of freedom, one axial, one rotational. The derivations for piezoelectric laminated plates are included in Appendix A. Comparisons of single versus multiple layer modeling, single layer piezoelectric modeling (mathematical versus. ABAQUS), piezoelectric laminated structures (mathematical versus ABAQUS), and equivalent loading versus deposition of surface charges were all conducted on a plate, as was done in the previous section on beams. For brevity, in this section only the results for the laminated structure will be shown.

The analysis began with three models of a plate subject to identical boundary conditions. One of the models was a laminated structure, generated in ABAQUS, composed of two layers of PVDF, and one layer of shape memory alloy. The piezoelectric models were generated in ABAQUS using twenty-node, three-dimensional continuum piezoelectric elements (C3D20RE), and the shape memory alloy layer was modeled using twenty-node, three-dimensional continuum elements (C3D20R). The second model was developed based on theoretical solutions in Matlab using a single-layer equivalent plate elements. The purpose of this model was to verify equivalent layer modeling techniques and theoretical piezoelectric modeling. The third model was developed in ABAQUS, using equivalent, eight-node, two-dimensional shell elements (S8R5) with equivalent loading conditions. The geometric and material properties are given in the following tables.

Table 4.15 Geometric properties of a piezoelectric laminated plate

Length	10 cm
Width	10 cm
PVDF thickness	0.05 cm (x2)
SMA thickness	0.05 cm
Total thickness	0.15 cm

Table 4.16 Material properties of a piezoelectric laminated plate

PVDF Elastic Modulus: (E)	2 Gpa (isotropic)
Piezoelectric stress coefficient: (e_{31}, e_{32})	-0.14 C/m^2
Dielectric constant: ($\in_{33}/\in_0$)	11.98
SMA Elastic Modulus (E)	6.95 Gpa (isotropic)

The simply supported plate was subjected to a distributed electrical surface charge of 1e6 C/m and the equivalent model with equivalent loading conditions. A plot of the results are shown in the following

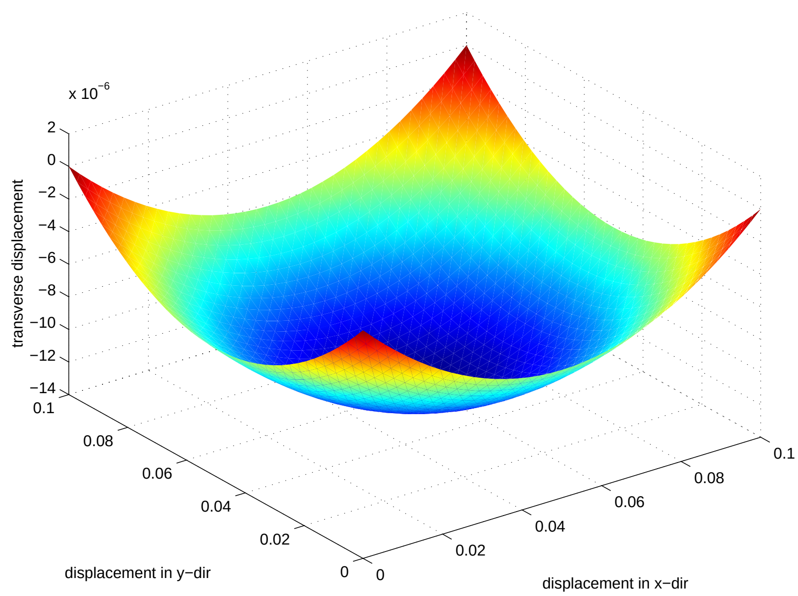

Figure 4.15 Results for a piezoelectric laminated plate subject to distributed surface charge

For clarity, the plot shown in figure 4.15, does not depict an overlay. The surface mesh was generated using the interpolations functions to include rotational degrees of freedom.

The results from the analysis were very similar to the beam analysis results. Numerical comparisons were made with the nodal displacements. The displacements coincide to four decimal digits with much less than 1% error.

CHAPTER 5

Summary, Conclusions, Contributions and Future Work

5.1 Summary and Conclusions

In summary, there were four major objectives of this thesis.

1.) Derive analytical solutions for laminated beams and plates and compare results to ABAQUS.
2.) Derive analytical solutions for piezoelectric beams and plates and compare results to ABAQUS.
3.) Derive analytical solutions for piezoelectric laminated beams and plates and compare results to ABAQUS.
4.) Determine equivalent electromechanical loading conditions to simulate electrical actuation and compare results to a equivalent models subjected to equivalent loading conditions.

All of the items have been addressed and are summarized as follows:

Item 1

Analytical solutions were derived for both beam and plate analysis based Kirchhoff's hypothesis and classical lamination theory. The equilibrium equations were derived by the principle of minimum potential energy. Finite element models were generated by deriving approximation functions that satisfy the geometric boundary conditions.

Multiple-layer models were developed in ABAQUS to compare single-layer theoretical solutions to the computational solutions. The analysis results in less than 1% difference in the solutions using single-layer modeling techniques to represent a multiple-layer structure. The results serve as justifications for modeling laminate structures as single layer equivalent structures.

Item 2

Analytical solutions that capture the electrical characteristics of the structure were derived for piezoelectric beams. The derivations were based on classical beam/plate theories, the principle of minimum potential energy, and the linear theory of piezoelectricity. Finite element models were developed, by deriving approximations functions on both mechanical and electrical degrees of freedom that satisfy the conditions at the boundaries.

A comparison of theoretical solutions with ABAQUS solutions using piezoelectric modeling capabilities resulted in a difference of less than 1%. The analysis provided a clear understanding of the electrical and mechanical characteristics of piezoelectric materials. The results provide justification for assumptions made by beam/plate theory and theory of piezoelectricity. The analysis also serves as the basis for modeling laminated structures and deriving equivalent loading techniques.

Item 3

Analytical solutions were derived for laminated piezoelectric beam and plates. The solutions were based on beam/plate theory, classical lamination theory, the principle of minimum potential energy, and the linear theory of piezoelectricity. Finite element models were developed, by deriving approximation functions for mechanical and electrical degrees of freedom such that the electrical degrees of freedom only exist within the piezoelectric layers.

A comparison the solutions with laminated piezoelectric structures using the piezoelectric modeling capabilities in ABAQUS resulted in less than 1% difference. The techniques greatly simplify the analysis of laminated beams and plates such that laminated piezoelectric structures can be modeled as single layer structures, which account for the electric and mechanical characteristics of the piezoelectric material. The analysis also serves as a basis for deriving equivalent electromechanical loading techniques to simulate electrical actuation within the piezoelectric layers.

Item 4

Equivalent mechanical loads were determined based on the theoretical solutions previously discussed and the linear theory of piezoelectricity. Through static condensation, piezoelectric models were used to calculate a displacement fields for a given electrical load, and the displacement fields were used to determine the required load to produce an identical response. Equivalent electromechanical loading techniques were also derived based on the constitutive equations of piezoelectricity. The method makes use of blocking forces due to piezoelectric actuation to calculate equivalent loading conditions based on the material and geometric properties of the structure.

Comparisons of equivalent single-layer models with equivalent loading conditions to laminated piezoelectric models generated using piezoelectric modeling capabilities in ABAQUS results in less than 1% difference. This techniques simplifies the analysis of piezoelectric beams and plates, so that the laminated structure can be modeled as a single layer, but it can be modeled with equivalent mechanical loads to simulate electrical actuation within the piezoelectric layers.

5.2 Contributions

- Demonstrated that multiple layer modeling is achievable by single layer equivalent modeling using equivalent material properties.
- Derived finite element methods for modeling piezoelectric structures, which account for mechanical and electrical characteristics of the structure.
- Validated the linear theory of piezoelectricity with ABAQUS models using piezoelectric elements.
- Demonstrated equivalent single layer techniques for modeling piezoelectric laminated structures.
- Determined equivalent loading techniques for modeling piezoelectric structures and piezoelectric laminated structures subject to electrical loading conditions.
- Simplified the analysis of piezoelectric laminated structures such that computational models can be developed to investigate the static and dynamic response using equivalent representations of the structure.

5.3 Future Work

The future works pertinent to the topic of this thesis may include

- Conducting an experiment to compare the results to theoretical and computational results.
- Deriving solutions that account for geometric and material nonlinearities.
- Extending the derivations to dynamic analysis for piezoelectric structures and piezoelectric laminated structures.
- Deriving solutions for time varying loads to simulate charge dissipation in the piezoelectric material.

Appendix A

A.1 Finite Element Formulations for Piezoelectric Plates

The finite element formulations for piezoelectric plates are derived based on energy methods, classical lamination theory, and the linear theory of piezoelectricity. The derivations are similar to the analysis of beams except additional degrees of freedom are introduced. The plane strain assumptions are no longer valid; hence, there are two additional degrees of per node. The interpolation functions are derived in a similar manner in which the functions were derived for the beam. The plate element is shown in Figure A.1.

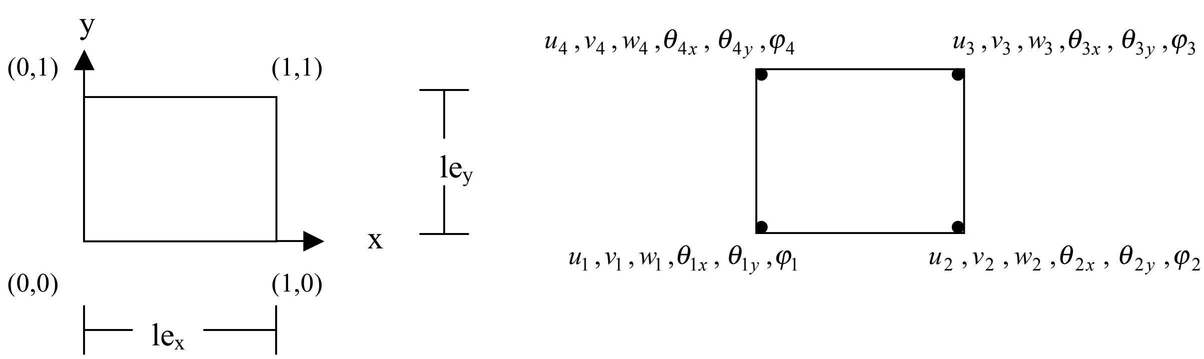

Figure A.1 Four node rectangular plate element

For axial displacements, we assume a bilinear polynomial of the following form,

$$\psi_i(x,y) = c_1 + c_2\,x + c_3\,y + c_4\,x\,y \qquad \text{(A.1)}$$

Solving the polynomial for the unknown constants given the boundary conditions derives the axial interpolations functions.

The interpolation functions are:

$$\begin{aligned}
&\psi_1 = (1-\eta)(1-\zeta),\ \psi_2 = (\eta)(1-\zeta),\\
&\psi_3 = (\zeta)(1-\eta),\quad \psi_4 = (\eta)(\zeta)\\
&for\ \ \eta = \frac{x}{le_x}\ \ ,\ \ \zeta = \frac{y}{le_y}\\
&Na = \{\psi_1\ ,\psi_2\ ,\psi_3\ ,\psi_4\}
\end{aligned} \qquad \text{(A.2)}$$

For transverse and rotational degree of freedom the polynomial approximation is given as follows,

$$\phi_i(x,y) = c_1 + c_2 x + c_3 y + c_4 x^2 + c_5 xy + c_6 y^2 + c_7 x^3 + c_8 x^2 y + c_9 xy^2 + c_{10} y^3 + c_{11} x^3 y + c_{12}\, xy^3$$

(A.3)

Solving the above equation for the unknown variable derives the interpolation functions for transverse and rotational degree of freedom which are given as, Transverse and rotational interpolation functions:

$$
\begin{aligned}
&\phi_1 = 1 - 3(\eta)^2 - (\eta)(\zeta) - 3(\zeta)^2 + 2(\eta)^3 + 3(\eta)^2(\zeta) + 3(\eta)(\zeta)^2 + 2(\zeta)^3 - 2(\eta)^3(\zeta) - 2(\zeta)^3(\eta) \\
&\phi_2 = (\zeta) - 2(\eta)(\zeta) - 2(\zeta)^2 + 2(\eta)(\zeta)^2 + (\zeta)^3 - (\zeta)^3(\eta) \\
&\phi_3 = -(\eta) + 2(\eta)^2 + (\eta)(\zeta) - (\eta)^3 - 2(\eta)^2(\zeta) + (\eta)^3(\zeta) \\
&\phi_4 = 3(\eta)^2 + (\eta)(\zeta) - 2(\eta)^3 - 3(\eta)^2(\zeta) - 3(\eta)(\zeta)^2 + 2(\eta)^3(\zeta) + 2(\zeta)^3(\eta) \\
&\phi_5 = (\eta)(\zeta) - 2(\eta)(\zeta)^2 + (\zeta)^3(\eta) \\
&\phi_6 = (\eta)^2 - (\eta)^3 - (\eta)^2(\zeta) + (\eta)^3(\zeta) \\
&\phi_7 = (\eta)(\zeta) + 3(\zeta)^2 - 3(\eta)^2(\zeta) - 3(\eta)(\zeta)^2 - 2(\zeta)^3 + 2(\eta)^3(\zeta) + 2(\zeta)^3(\eta) \\
&\phi_8 = -(\zeta)^2 + (\eta)(\zeta)^2 + (\zeta)^3 - (\zeta)^3(\eta) \\
&\phi_9 = -(\eta)(\zeta) + 2(\eta)^2(\zeta) - (\eta)^3(\zeta) \\
&\phi_{10} = -(\eta)(\zeta) + 3(\eta)^2(\zeta) + 3(\eta)(\zeta)^2 - 2(\eta)^3(\zeta) - 2(\zeta)^3(\eta) \\
&\phi_{11} = -(\eta)(\zeta)^2 + (\zeta)^3(\eta) \\
&\phi_{12} = (\eta)^2(\zeta) - (\eta)^3(\zeta) \\
&for\ \ \eta = \frac{x}{le_x}\ \ ,\ \ \zeta = \frac{y}{le_y} \\
&N_t = \{\phi_1, \phi_2, \phi_3, \phi_4, \phi_5, \phi_6, \phi_7, \phi_8, \phi_9, \phi_{10}, \phi_{11}, \phi_{12}\}
\end{aligned}
\tag{A.4}
$$

The interpolations functions for electric potential through the thickness are given as follows,

$$
\begin{aligned}
&\xi^*_{1_1} = \frac{1}{2} + \beta\ \ ,\ \ \xi^*_{2_2} = \frac{1}{2} - \beta \\
&for\ \ \beta = \frac{z}{he} \\
&N_{e_e}^* = \{\xi^*_1, \xi^*_{2_2}\}
\end{aligned}
\tag{A.5}
$$

Zero electrical potential boundary conditions are imposed on the bottom surface. The electric potential may vary across the element boundaries, as well as through the thickness, therefore the will be functions of the three dimensions of the plate. The product of axial and through the thickness interpolation functions produces the interpolation function for the electric potentials as follows,

$$N_e = N_a N_e^* = \{ (1-\eta)(1-\zeta),\ (\eta)(1-\zeta),\ \zeta(1-\eta),\ (\eta)(\zeta)\}\left\{\frac{1}{2}+\beta\right\}$$

$$\xi_1 = \left(\frac{1}{2}+\beta\right)(1-\eta)(1-\zeta),\ \ \xi_2 = \left(\frac{1}{2}+\beta\right)(\eta)(1-\zeta)$$

$$\xi_3 = \left(\frac{1}{2}+\beta\right)(\zeta)(1-\eta),\qquad \xi_4 = \left(\frac{1}{2}+\beta\right)(\eta)(\zeta) \tag{A.6}$$

$$for\ \ \beta = \frac{z}{he},\ \eta = \frac{x}{le_x},\ \ \zeta = \frac{y}{le_y}$$

$$N_e = \{\xi_1,\ \xi_2, \xi_3, \xi_4\}$$

For plate analysis the plane strain assumption is not valid; hence the displacement field and stress will be as follows:

Displacement field:

$$u(x,y,z) = u^o(x,y) - z\frac{\partial w^o(x,y)}{\partial x} \tag{A.7}$$

$$v(x,y,z) = v^o(x,y) - z\frac{\partial w^o(x,y)}{\partial y} \tag{A.8}$$

$$w(x,y,z) = w^o(x,y) \tag{A.9}$$

Strain:

$$\varepsilon_x(x,y,z) \equiv \frac{\partial u(x,y,z)}{\partial x} = \frac{\partial u^o(x,y)}{\partial x} - z\frac{\partial^2 w^o(x,y)}{\partial x^2} \tag{A.10}$$

$$\varepsilon_y(x,y,z) \equiv \frac{\partial v(x,y,z)}{\partial y} = \frac{\partial v^o(x,y)}{\partial y} - z\frac{\partial^2 w^o(x,y)}{\partial y^2} \tag{A.11}$$

$$\gamma_{xy}(x,y,z) \equiv \frac{\partial u^o(x,y)}{\partial x} + \frac{\partial v^o(x,y)}{\partial y} - 2z\frac{\partial^2 w^o(x,y)}{\partial x \partial y} \tag{A.12}$$

The derivations are based on energy methods and variational principle, the stain energy for the piezoelectric plate is given as,

$$V = -\int_V \left[\frac{1}{2} c_{ijkl} S_{ij} S_{kl} - e_{ijk} E_i S_{jk} - \frac{1}{2} \varepsilon_{ij} E_i E_j \right] dV \tag{A.13}$$

Substituting the expressions for the strains in the above equation and taking the first variation, with respect to the axial, transverse, and electric potential results in the following:

$$\begin{aligned}
\delta V = &\int_V \left[Q_{11}\left(\frac{\partial u}{\partial x} - z\frac{\partial^2 w}{\partial x^2} \right) + Q_{12}\left(\frac{\partial v}{\partial y} - z\frac{\partial^2 w}{\partial y^2} \right) - e_{31}\left(-\frac{\partial \varphi}{\partial z} \right) \right] \delta\left(\frac{\partial u}{\partial x} - z\frac{\partial^2 w}{\partial x^2} \right) dV + \\
&\int_V \left[Q_{21}\left(\frac{\partial u}{\partial x} - z\frac{\partial^2 w}{\partial x^2} \right) + Q_{22}\left(\frac{\partial v}{\partial y} - z\frac{\partial^2 w}{\partial y^2} \right) - e_{32}\left(-\frac{\partial \varphi}{\partial z} \right) \right] \delta\left(\frac{\partial v}{\partial y} - z\frac{\partial^2 w}{\partial y^2} \right) dV + \\
&\int_V \left[Q_{66}\left(\frac{\partial u}{\partial x} + \frac{\partial v}{\partial y} - 2z\frac{\partial^2 w}{\partial x \partial y} \right) - e_{36}\left(-\frac{\partial \varphi}{\partial z} \right) \right] \delta\left(\frac{\partial u}{\partial x} + \frac{\partial v}{\partial y} - 2z\frac{\partial^2 w}{\partial x \partial y} \right) dV - \\
&\int_V \left[e_{31}\left(\frac{\partial u}{\partial x} - z\frac{\partial^2 w}{\partial x^2} \right) + e_{32}\left(\frac{\partial v}{\partial y} - z\frac{\partial^2 w}{\partial y^2} \right) - e_{36}\left(\frac{\partial u}{\partial x} + \frac{\partial v}{\partial y} - 2z\frac{\partial^2 w}{\partial x \partial y} \right) + \kappa_o\left(-\frac{\partial \varphi}{\partial z} \right) \right] \delta\left(-\frac{\partial \varphi}{\partial z} \right) dV
\end{aligned} \tag{A.14}$$

The approximation functions are given as,

$$\begin{aligned}
u(x) &= \sum_{i=1}^{4} \psi_i\, u_i \\
v(y) &= \sum_{i=1}^{4} \psi_i\, v_i \\
w(x) &= \sum_{i=1}^{12} \phi_i\, w_i \\
\varphi\,(x, y, z) &= \sum_{i=1}^{2} \xi_i \varphi_i
\end{aligned} \tag{A.15}$$

Upon substitution of the approximation functions, the element stiffness matrix is defined as

$$K_{ij}^{11} = \int_V \left[Q_{11}\left(\frac{\partial \psi_j^e}{\partial x}\frac{\partial \psi_i^e}{\partial x} \right) + Q_{66}\left(\frac{\partial \psi_j^e}{\partial y}\frac{\partial \psi_i^e}{\partial y} \right) \right] dV$$

$$K_{ij}^{12} = \int_V \left[Q_{12}\left(\frac{\partial \psi_j^e}{\partial x}\frac{\partial \psi_i^e}{\partial y} \right) + Q_{66}\left(\frac{\partial \psi_j^e}{\partial y}\frac{\partial \psi_i^e}{\partial x} \right) \right] dV$$

$$K_{ij}^{13} = -\int_V z\left[Q_{11}\left(\frac{\partial \psi_j^e}{\partial x}\frac{\partial^2 \phi_i^e}{\partial x^2} \right) + Q_{12}\left(\frac{\partial \psi_j^e}{\partial x}\frac{\partial^2 \phi_i^e}{\partial y^2} \right) + 2Q_{66}\left(\frac{\partial \psi_j^e}{\partial y}\frac{\partial^2 \phi_i^e}{\partial x \partial y} \right) \right] dV$$

$$K_{ij}^{14} = \int_V \left[e_{31}\left(\frac{\partial \psi_j^e}{\partial x}\frac{\partial \xi_i^e}{\partial z} \right) + e_{36}\left(\frac{\partial \psi_j^e}{\partial y}\frac{\partial \xi_i^e}{\partial z} \right) \right] dV$$

$$K_{ij}^{21} = \int_V \left[Q_{21}\left(\frac{\partial \psi_j^e}{\partial y}\frac{\partial \psi_i^e}{\partial x} \right) + Q_{66}\left(\frac{\partial \psi_j^e}{\partial x}\frac{\partial \psi_i^e}{\partial y} \right) \right] dV$$

$$K_{ij}^{22} = \int_V \left[Q_{22}\left(\frac{\partial \psi_j^e}{\partial y}\frac{\partial \psi_i^e}{\partial y} \right) + Q_{66}\left(\frac{\partial \psi_j^e}{\partial x}\frac{\partial \psi_i^e}{\partial x} \right) \right] dV$$

$$K_{ij}^{23} = -\int_V z\left[Q_{12}\left(\frac{\partial \psi_j^e}{\partial y}\frac{\partial^2 \phi_i^e}{\partial x^2} \right) + Q_{22}\left(\frac{\partial \psi_j^e}{\partial y}\frac{\partial^2 \phi_i^e}{\partial y^2} \right) + 2Q_{66}\left(\frac{\partial \psi_j^e}{\partial x}\frac{\partial^2 \phi_i^e}{\partial x \partial y} \right) \right] dV$$

$$K_{ij}^{24} = \int_V \left[e_{32}\left(\frac{\partial \psi_j^e}{\partial y}\frac{\partial \xi_i^e}{\partial z} \right) + e_{36}\left(\frac{\partial \psi_j^e}{\partial x}\frac{\partial \xi_i^e}{\partial z} \right) \right] dV$$

$$K_{ij}^{31} = -\int_V z\left[Q_{11}\left(\frac{\partial^2 \phi_i^e}{\partial x^2}\frac{\partial \psi_i^e}{\partial x} \right) + Q_{12}\left(\frac{\partial^2 \phi_i^e}{\partial y^2}\frac{\partial \psi_i^e}{\partial x} \right) + 2Q_{66}\left(\frac{\partial^2 \phi_i^e}{\partial x \partial y}\frac{\partial \psi_i^e}{\partial y} \right) \right] dV$$

$$K_{ij}^{32} = -\int_V z\left[Q_{21}\left(\frac{\partial^2 \phi_i^e}{\partial x^2}\frac{\partial \psi_i^e}{\partial y} \right) + Q_{22}\left(\frac{\partial^2 \phi_i^e}{\partial y^2}\frac{\partial \psi_i^e}{\partial y} \right) + 2Q_{66}\left(\frac{\partial^2 \phi_i^e}{\partial x \partial y}\frac{\partial \psi_i^e}{\partial x} \right) \right] dV$$

$$K_{ij}^{33} = \int_V z^2 \left[\begin{array}{l} Q_{11}\left(\frac{\partial^2 \phi_i^e}{\partial x^2}\frac{\partial^2 \phi_i^e}{\partial x^2} \right) + Q_{12}\left(\frac{\partial^2 \phi_i^e}{\partial x^2}\frac{\partial^2 \phi_i^e}{\partial y^2} \right) + Q_{21}\left(\frac{\partial^2 \phi_i^e}{\partial y^2}\frac{\partial^2 \phi_i^e}{\partial x^2} \right) \\ Q_{22}\left(\frac{\partial^2 \phi_i^e}{\partial y^2}\frac{\partial^2 \phi_i^e}{\partial y^2} \right) + 4Q_{66}\left(\frac{\partial^2 \phi_i^e}{\partial x \partial y}\frac{\partial^2 \phi_i^e}{\partial x \partial y} \right) \end{array} \right] dV$$

$$K_{ij}^{34} = -\int_V z\left[e_{31}\left(\frac{\partial^2 \phi_i^e}{\partial x^2}\frac{\partial \xi_i^e}{\partial z} \right) + e_{32}\left(\frac{\partial^2 \phi_i^e}{\partial y^2}\frac{\partial \xi_i^e}{\partial z} \right) + 2e_{36}\left(\frac{\partial^2 \phi_i^e}{\partial x \partial y}\frac{\partial \xi_i^e}{\partial z} \right) \right] dV$$

$$K_{ij}^{41} = \int_V \left[e_{31}\left(\frac{\partial \xi_i^e}{\partial z}\frac{\partial \psi_j^e}{\partial x} \right) + e_{36}\left(\frac{\partial \xi_i^e}{\partial z}\frac{\partial \psi_j^e}{\partial y} \right) \right] dV$$

$$K_{ij}^{42} = \int_V \left[e_{32}\left(\frac{\partial \xi_i^e}{\partial z}\frac{\partial \psi_j^e}{\partial y} \right) + e_{36}\left(\frac{\partial \xi_i^e}{\partial z}\frac{\partial \psi_j^e}{\partial x} \right) \right] dV$$

$$K_{ij}^{43} = -\int_V z\left[e_{31}\left(\frac{\partial \xi_i^e}{\partial z}\frac{\partial^2 \phi_i^e}{\partial x^2} \right) + e_{32}\left(\frac{\partial \xi_i^e}{\partial z}\frac{\partial^2 \phi_i^e}{\partial y^2} \right) + 2e_{36}\left(\frac{\partial \xi_i^e}{\partial z}\frac{\partial^2 \phi_i^e}{\partial x \partial y} \right) \right] dV$$

$$K_{ij}^{44} = -\int_V \left[\kappa_o\left(\frac{\partial \xi_i^e}{\partial z}\frac{\partial \xi_i^e}{\partial z} \right) \right] dV \qquad \text{(A.16)}$$

The external work is given as,

$$W_{total} = \iint_R \left[t_x\left(u - z\frac{dw}{dx}\right) + t_y\left(v - z\frac{dw}{dy}\right) + f_t w - \sigma\varphi \right] dx\,dy + \iint_R \left[f_{a_x} u\right] dy\,dz + \iint_R \left[f_{a_y} v\right] dx\,dz \tag{A.17}$$

Taking the first variation with respect to the axial and transverse displacements, and the electric potential, the virtual work is,

$$\begin{aligned} \delta W_{total} = & \iint_R \left[\psi_j t_x\right]\delta u_i\, dx\,dy + \iint_R \left[\psi_j f_{a_x}\right]\delta u_i\, dy\,dz + \iint_R \left[\psi_j t_y\right]\delta v_i\, dx\,dy + \iint_R \left[\psi_j f_{a_y}\right]\delta v_i\, dx\,dz - \\ & \iint_R \left[\xi_j \sigma\right]\delta \varphi_i\, dx\,dy + \iint_R \left[\phi_j f_t - z\frac{d\phi_j}{dx}t_x - z\frac{d\phi_j}{dy}t_y\right]\delta w_i\, dx\,dy \end{aligned} \tag{A.18}$$

The resultant force vector is defined as follows,

$$\begin{aligned} F_{ij}^1 &= \iint_R \left[\psi_j t_x\right] dx\,dy + \iint_R \left[\psi_j f_{a_x}\right] dy\,dz \\ F_{ij}^2 &= \iint_R \left[\psi_j t_y\right] dx\,dy + \iint_R \left[\psi_j f_{a_y}\right] dx\,dz \\ F_{ij}^3 &= \iint_R \left[\phi_j f_t - z\frac{d\phi_j}{dx}t_x - z\frac{d\phi_j}{dy}t_y\right] dx\,dy \\ F_{ij}^4 &= -\iint_R \left[\xi_j \sigma\right] dx\,dy \end{aligned} \tag{A.19}$$

Based on minimum energy principles the static equilibrium equations are given as,

$$\begin{bmatrix} K_{11}^e & K_{12}^e & K_{13}^e & K_{14}^e \\ K_{21}^e & K_{22}^e & K_{23}^e & K_{24}^e \\ K_{31}^e & K_{32}^e & K_{33}^e & K_{34}^e \\ K_{41}^e & K_{42}^e & K_{43}^e & K_{44}^e \end{bmatrix} \begin{Bmatrix} u \\ v \\ w \\ \varphi \end{Bmatrix} = \begin{Bmatrix} F_1^e \\ F_2^e \\ F_3^e \\ F_4^e \end{Bmatrix} \tag{A.20}$$

Bibliography

[1] Almeida, Sergio Franscino Muller de. Shape Control of Laminated Plates with Piezoelectric Actuators Including Stress-Stiffening Effects. *AIAA Journal*, Vol. 37, No. 8, March 1999

[2] Bakish, Robert. *Electron Beam Technology.* John Wiley & Sons, Inc., 1962.

[3] Bhattacharya, P., Suhail, H., and Sinha, P.K., Finite Element Free Vibration Analysis of Smart Laminated Composite Beams and Plates. *Journal of Intelligent Material Systems and Structures*, Vol. 9, January 1998.

[4] Budynas, Richard G. *Advanced Strength and Applied Stress Analysis.* McGraw-Hill, 1977.

[5] Che, Su-Huan, Guo-Feng, Yao, and Cheng Huang. A New Intelligent Thin-shell Element. *Smart Material Structures,* 9 (2000) 10-18.

[6] Cheng, Zhen-Qiang; Lim, C.W.; and Kitipornchai, S. Three-Dimensional Asymptotic Approach to Inhomogeneous and Laminated Piezoelectric Plates. *International Journal of Solids and Structures,* 37 (2000), pp. 3153-3175.

[7] Donnell, Lloyd Hamilton. *Beams, Plates, and Shells.* McGraw-Hill, Inc., 1973.

[8] Dyn, Clive L., and Shames, Irving H. *Solid Mechanics: A Variational Approach.* McGraw-Hill, Inc., 1973.

[9] Gopinathan, Senthil V., Vasundra V. A Review and Critique of Theories for Piezoelectric Laminates. *Smart Material Structures* 9 (2000) 24-48.

[10] Henno, Allik and Huges, Thomas J.R. Finite Element Method for Piezoelectric Vibration. *International Journal for Numerical Methods in Engineering*, Vol. 2, pp. 151-157, 1970.

[11] Heyliger, P. and Brooks, S. Exact Solutions for Laminated Piezoelectric Plates in Cylindrical Bending. *ASME Jornal of Applied Mechanics,* December 1996, Vol. 63. Pp. 903-910.

[12] Huang, Y-Q, Liu, M., and Wu, C-C. Bimaterial Interface Hybrid Element for Piezoelectric Laminated Analysis. *Journal of Strain Analysis*, Vol. 34, No. 2. January 1999.

[13] Hyer, Michael W. *Stress Analysis of Fiber-Reinforced Composite Materials*. McGraw-Hill, Inc., 1998.

[14] Jones, Robert M. *Mechanics of Composite Materials.* Hemisphere Publishing Corporation, 1975.

[15] Lam, K.Y., and Ng T.Y. Active Control of Composite Plates with Intelligent Piezoelectric Sensors and Actuators under Various Dynamics Loading Conditions. *Smart Material Structures*, Vol. 8, 1999, pp. 223-237.

[16] Low, T.S. and Guo, W. Modeling of a Three-Layer Piezoelectric Bimorph Beam with Hysteresis. *Journal of Microelectromechanical Systems*, Vol. 4, No. 4, December 1995.

[17] Main, John A., Nelson, George, and Martin, Jeffrey. Electron Gun Control of Smart Materials. *SPIE Conference on Smart Structures and Integrated Systems*. SPIE Vol. 3329, pp. 688-693.

[18] Main, John A., Nelson, George, and Martin, Jeffrey. Maintenance of Inflated Structure Shape Using Electron Gun Controlled Piezoelectric Materials. *The American Institute of Aeronautics and Astronautics*, 1998, pp. 2294-2301. AIAA-98-1982.

[19] Main, John A., Nelson, George, and Martin, Jeffrey. Noncontact Shape Control of Membrane Mirrors. *Ultralightweight Space Optics Challenge Workshop*. March 24-25, 1999. Napa, California.

[20] Main, John A., Nelson, George, and Martin, Jeffrey. Shape Control of Deployable Membrane Mirrors. *International Mechanical Engineering Congress and Exposition,* November 15-10, 1998, Anaheim, California. AD Vol 57/MD-Vol. 83. Adaptive Structures and Material Systems, pp. 217-223.

[21] Meirovitch, Leonard. *Analytical Methods in Vibrations.* Macmillan Company, 1967.

[22] Meitovitch, Leonard. *Principles and Techniques of Vibrations*. Prentice-Hall, Inc., 1997.

[23] Morgan Electo Ceramics. Cantilever Mounted PZT 5A Bimorphs. *Technical Publication TP-245*, Morgan Electro Ceramics Web Site, URL: www.morgan-electoceramics.com

[24] Morgan Electro Ceramics. C.P. Germano. Piezoelectricity: On the Meaning of "g" and "d" Constant as Applied to Simple Piezoelectric Modes of Vibration. *Technical Publication TP-222*, Morgan Electro Ceramics Web Site, URL: www.morgan-electoceramics.com, Engineering Memorandum No. 61-15.

[25] Morgan Electro Ceramics. Ceramic Bender Bimorphs. Useful Relationships for Ceramic Bender Bimorphs. *Technical Publication TP-223*, Morgan Electro Ceramics Web Site, URL: www.morgan-electoceramics.com

[26] Morgan Electro Ceramics. Robert Gerson. Piezoelectric Coupling. On the Meaning of Piezoelectric Coupling. *Technical Publication TP-224*, Morgan Electro Ceramics Web Site, URL: www.morgan-electoceramics.com

[27] Reddy, J.N. *Mechanics of Laminated Composite Plates*. CRC Press, 1997.

[28] Reddy, J.N. *An Introduction to the Finite Element Method.* McGraw-Hill, Inc., 1993.

[29] Richards, T. H. *Energy Methods in Stress Analysis.* Ellis Horwood, 1977.

[30] Saravanos, Dimitris A. Mixed Laminate Theory and Finite Element for Smart Piezoelectric Composite Shell Structures. *AIAA Journal*, Vol. 35, No. 8, August 1997.

[31] Savravanos, Dimitris A., Heyliger, Paul R., and Hopkins, Dale A. Layerwise Mechanics and Finite Element for the Dynamic Analysis of Piezoelectric Composite Plates. *International Journal of Solid Structures*, Vol 34, No. 3, pp. 359-378, 1997.

[32] Sessler, G.M. Piezoelectricity in Polyvinylidene Fluoride. *J. Acoust. Soc. Am.* 70(6), Dec. 1981, pp. 1598-1608.

[33] Shames, Irving H. and Dym, Clive L. *Energy and Finite Element Methods in Structural Mechanics.* Hemisphere Publishing Corporation, 1985.

[34] Suleman, A. and Venkayya, V.B. A Simple Finite Element Formulation for a Laminated Composite Plate with Piezoelectric Layers. *Journal of Intelligent Material Systems and Structures,* Vol 6, November 1995.

[35] Sun, Dongchang, Wang, Dajun, Xu, Z.L., and Hongxin, Wu. Distributed Piezoelectric Element Method for Vibration Control of Smart Plates. *AIAA Journal*, Vol. 37, No. 11, November 1999.

[36] Tiersten, H.F. Electroelastic equations for Electroded thin Plates subjected to Large Driving Voltages. *Journal of Applied Physics*, Vol. 74, No. 5, September 1993.

[37] Tiersten, H.F. *Linear Piezoelectric Plate Vibrations.* Plenum Publishing Corporation, 1969.

[38] Tzou, H.S. and J.P Zhong. Electromechanics and Vibrations of Piezoelectric Shell Distributed Systems. *Jornal of Dynamic Systems, Measurement and Control*, Vol 115, pp. 506-516. Sept 1993.

[39] Weinberg, Marc S. Working Equations for Piezoelectric Actuators and Sensors. *Journal of Microelectromechanical Systems*, Vol. 8, No. 4, December 1999, pp. 529-533.

[40] Weinberg, Marc S. Working Equations for Piezoelectric Actuators and Sensors. *Journal of Microelectromechanical Systems*, Vol. 8, No. 4, December 1999.

[41] Zhou, Y.S. and Tiersten, H.F. An Elastic Analysis of Laminated Composite Plates in Cylindrical Bending due to Piezoelectric Actuators. *Smart Material Structures* 3, 225-265.

Vita

Clayton Levon Smith was born February 22,1973, in Baton Rouge, Louisiana, the second child of Clifford and Carolyn Smith. He graduated from the Georgia Institute of Technology in August 1998, with a Bachelor of Mechanical Engineering and from Albany State University in May 1999, with a Bachelor of Arts in Mathematics. Clayton has served nine years in the Army National Guard while attending school and worked, one year, for General Physics Corporation at Merck Inc., Albany, Ga. He began graduate studies at Virginia Polytechnic Institute and State University in August 1999, under the supervision of Professor Daniel J. Inman. As of January 2001, Clayton has been a Ph.D. student at Clemson University under the supervision of Professor Eric M. Austin. Upon graduation, Clayton plans to continue doctoral studies at Clemson University.

Clayton L. Smith